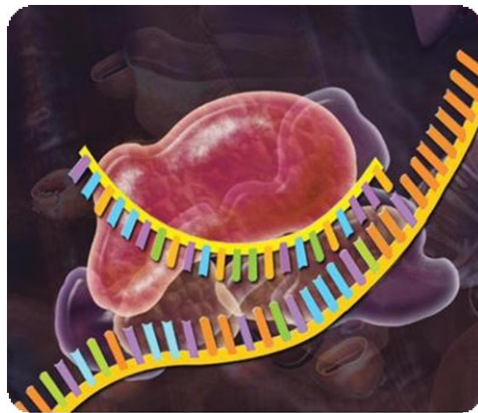




UNIVERSITA' DI NAPOLI FEDERICO II

**DOTTORATO DI RICERCA IN BIOCHIMICA
E BIOLOGIA MOLECOLARE E CELLULARE
XXIII CICLO**

microRNA in cellular senescence



Candidate: Dott.ssa Carla SEDIA

Tutor: Prof.ssa Raffaella FARAONIO



UNIVERSITA' DI NAPOLI "FEDERICO II"

**DOTTORATO DI RICERCA
BIOCHIMICA E BIOLOGIA MOLECOLARE E CELLULARE
XXIII CICLO**

microRNA in cellular senescence

**Candidate
Carla Sedia**

Tutor
Prof. Raffaella Faraonio

Coordinator
Prof. Paolo Arcari

Academic Year 2010/2011

RINGRAZIAMENTI E DEDICHE

I would like to thank Prof. Filiberto Cimino for giving me the opportunity to join his group;

I thank prof.ssa Raffaella Faraonio for her tutorship in these years.

I wish to thank dott.ssa Fabiana Passaro for her great enthusiasm and for enlightening scientific discussions.

A special thank goes to prof. Massimo Santoro and his group at the Dipartimento di Patologia e Biologia Cellulare e Molecolare. I profited a lot from discussions with the members of his group; in particular I wish to thank dott. Paolo Salerno.

I also want to thank the colleagues that work in the Dipartimento di Biochimica e Biotecnologie Mediche for their sustaining, friendship and instructive scientific discussions and in particular Camilla and Maria Luigia who has been a friend more than a colleague and support in times of difficulty and an ally in times of joy.

I am especially grateful to my mother AnnaMaria, that has supported my dreams and aspirations giving me the privilege of the study, my father Luigi for having faith in me and for giving me the tough and durable character that has allowed me to overcome many obstacles, my brother Sergio and his family, in particular Michelle and Karen for having delighted these three years with their birth.

I would like to thank *Madonna's tribe* for having welcomed me as a member of their family and for the serenity and joy that they infuse in me. Finally, these three years of doctoral study have made a gift to me. Thanks to Gabriele: his smile is my smile (thanks for the technical support with pc, too).

He has taught me how to compose a puzzle: arrange the pieces one at a time, very patiently. The pieces of a puzzle, the pieces of an experiment, the pieces of my life.

*“We refuse to be
What you wanted us to be;
We are what we are:
That's the way it's going to be. You don't know”*

Ai miei due sborbottoni

SUMMARY

Senescence is recognized as a permanent arrest of cell proliferation triggered by telomere shortening or various stresses. Senescence imposes a barrier to tumorigenesis and contributes to aging. It represents a cell response that encompasses gene expression regulation at transcriptional and post-transcriptional levels. MicroRNAs (miRNAs or miRs) are small non-coding RNAs that regulate diverse biological processes through their control of mRNA degradation or translation.

In this work, we have analyzed the expression profiles of 284 known microRNAs in senescent relative to early-passage IMR90 human diploid fibroblasts. We found that 179 microRNAs were expressed at significant level and that in senescent cells 47% were downregulated (at least 2-fold) and 19% were upregulated at same extent.

With only few exceptions, a similar expression profile was observed in human senescent BJ fibroblasts, as well as in young IMR90 fibroblasts treated with a mild chronic oxidative stress or with etoposide. The upregulated microRNAs, validated by Quantitative Real Time PCR, included miR-23b, miR-30e-5p, miR-126*, miR-134, miR-200c, miR-210, miR-376a*, miR-369-5p, miR-379, miR-410, miR-432, miR-485-5p, miR-486, miR-494, miR-542-5p, miR-654, miR-656 and some of them (miR-134, miR-369-3p, miR-376a*, miR-379, miR-410, miR-432, miR-485-5p, miR-494, miR-654 and miR-656) are members of an imprinted region of human chromosome 14.

We found that ectopic expression of some of the upregulated microRNAs (miR-210, miR-376a*, miR-486, miR-494, miR-542-5p, miR-654) in young proliferating fibroblasts triggers a premature senescent phenotype showing typical markers of senescence and accompanied also by the appearance of molecular complexes involved in different patterns of DDR (DNA damage response).

RIASSUNTO

La senescenza cellulare viene riconosciuta come un arresto permanente della proliferazione cellulare dovuto all'accorciamento dei telomeri o anche ad altri tipi di stress. La senescenza cellulare è considerata un meccanismo di soppressione tumorale e contribuisce all'invecchiamento dell'organismo. Rappresenta, altresì, una risposta cellulare che coinvolge la regolazione dell'espressione genica a livello trascrizionale e post-trascrizionale. I microRNA (miRNA o miR) sono una classe di piccoli RNA non codificanti che regolano diversi processi biologici attraverso il controllo della traduzione o degradazione dell'mRNA target.

In questo lavoro abbiamo confrontato il profilo di espressione di 284 microRNA umani noti in cellule IMR90 senescenti in seguito a ripetute duplicazioni in vitro rispetto a cellule giovani. Abbiamo così trovato che 179 microRNA sono espressi in questa linea cellulare a livelli significativi e che il 47% di essi è presente a livelli più bassi in cellule senescenti rispetto a quelle giovani mentre il 19% risulta presente a livelli più alti (almeno di due volte).

Un profilo di espressione pressoché identico, con poche eccezioni, è stato riscontrato in cellule BJ senescenti così come in IMR90 giovani trattate con stress ossidativo cronico moderato o con Etoposide. I microRNA iper-espressi risultanti dallo screening e dalle successive validazioni con PCR Real Time quantitativa sono: miR-23b, miR-30e-5p, miR-126*, miR-134, miR-200c, miR-210, miR-376a*, miR-369-5p, miR-379, miR-410, miR-432, miR-485-5p, miR-486, miR-494, miR-542-5p, miR-654, miR-656 e alcuni di essi (miR-134, miR-369-3p, miR-376a*, miR-379, miR-410, miR-432, miR-485-5p, miR-494, miR-654 e miR-656) appartengono ad un'unica regione cromosomica localizzata sul cromosoma 14 umano.

Noi abbiamo trovato che l'espressione ectopica di alcuni microRNA risultati iper-espressi in senescenza (miR-210, miR-376a*, miR-486, miR-494, miR-542-5p, miR-654) in cellule IMR90 giovani induce la comparsa di un fenotipo senescente prematuro che mostra i tipici marcatori della senescenza accompagnato anche dalla comparsa di alcuni complessi molecolari associati al DDR (DNA damage response).

INDEX

	Pag.
1. INTRODUCTION	1
1.1 Cellular senescence	5
1.2 Molecular mechanisms of cellular senescence	5
1.2.1 The p53 pathway	5
1.2.2 The p16 ^{INK4a} pathway	9
1.3 Causes of senescence	10
1.3.1 Telomere dysfunction	10
1.3.2 Oxidative stress	11
1.3.3 DNA-damage induced by drugs	12
1.3.4 Oncogene-induced senescence (OIS)	13
1.4 MicroRNAs	14
1.5 Biological role of microRNAs in senescence	18
1.6 Scientific hypothesis and aim of work	18
2. MATERIALS AND METHODS	20
2.1 Cell cultures and replicative senescence	20
2.2 Induction of premature senescence in IMR90 cells by treatment with Diethylmaleate (DEM) and etoposide	20
2.3 RNA extraction and real time PCR for mRNA	21
2.4 RNA extraction and analysis of human microRNAs expression	22
2.5 Quantitative PCR Real-Time for microRNAs	23
2.6 Transfection of IMR90 cells by electroporation	23
2.7 Bromodeoxyuridine assay.	24
2.8 Assay for β -galactosidase activity in situ	24
2.9 Comet assay	25
2.10 Western blot analysis	25
3. RESULTS	27
3.1 Characterization of replicative senescence in IMR90	27
3.2 microRNA expression profiles in senescent IMR90 fibroblasts	29
3.3 Validation of microRNA profile in senescent IMR90 fibroblasts	31
3.4 Senescence-associated microRNA profiles in BJ cells and in premature senescent IMR90 cells	33
3.5 Overexpression of some selected up-regulated microRNAs inhibits cell growth in IMR90 cells	37
3.6 Overexpression of some selected microRNAs induces a senescent-like phenotype	41
3.7 Senescent-like phenotype is related to a persistent DNA damage	43
3.8 Prediction of targets of Senescence-Associated microRNAs (SA-	

<i>microRNAs) involved in pathway correlated to cellular senescence</i>	45
4. DISCUSSION/CONCLUSIONS	47
5. REFERENCES	49

LIST OF TABLES AND FIGURES

Table 1. microRNA expression profile in senescent IMR90 fibroblasts	30
Table 2. Validation of senescence-associated microRNA profiles in IMR90 cells	32
Table III. Senescence-associated microRNA profiles in BJ cells	34
Table IV. Senescence-associated microRNA profiles in premature senescent IMR90 cells	36
Table V. Prediction of targets of Senescence-Associated microRNAs (SA-microRNAs)	46
Figure 1. Causes of senescence and main features of senescent cells	2
Figure 2. Signaling pathways leading to cellular senescence	6
Figure 3. The DNA -damage response (DDR).	8
Figure 4. Biogenesis of microRNAs	16
Figure 5. Characterization of replicative senescence in IMR90	28
Figure 6. Senescence-associated microRNA profiles in BJ cells	34
Figure 7. Senescence-associated microRNA profiles in premature senescent IMR90 cells	36
Figure 8. Overexpression of some selected up-regulated microRNAs inhibits cell growth in IMR90 cells	38
Figure 9. Bromodeoxyuridine (BrdU) labeling in cells over-expressing selected microRNAs	40
Figure 10. Overexpression of some selected microRNAs induces a senescent-like phenotype	42
Figure 11. Senescent-like phenotype is related to activation of a persistent DNA damage	44

1. INTRODUCTION

1.1 *Cellular senescence*

Cellular senescence is an irreversible arrest of cell proliferation that occurs in somatic cells within multicellular organisms and is caused by loss of replicative potential. Senescent cells are metabolically active but because they lack the capacity to replicate, are unable to perform DNA synthesis and continue to grow (1).

Therefore cellular senescence has been considered as a model of mammalian aging. The term “cellular senescence” was used for the first time in 1960s by Hayflick and Moorhead to describe the inevitable and irreversible proliferation arrest of primary human cells in culture, a phenomenon known as the “Hayflick limit”(2). They reported the inability of normal human diploid cells to undergo further replication in spite of physiological mitogenic stimuli after a finite numbers of divisions; this type of senescence was defined *replicative senescence*. Before then, it was believed that cellular senescence was an artefact due to culture conditions, until a series of findings demonstrated that aging of cells is an intrinsic phenomenon, specific for each cell type *in vitro* and *in vivo*. Hayflick and Moorhead worked with fibroblasts, a cell type found in connective tissues, but replicative senescence has been found in other cell types: keratinocytes, endothelial cells, lymphocytes, adrenocortical cells, vascular smooth muscle cells, chondrocytes, but with different characteristics. The replicative senescence described by Hayflick and colleagues results, at least in part, from telomere shortening. In normal human fibroblast cells, telomeres become progressively shorter with each population doubling until they reach a critically short length. Critically short telomeres are only one of signals that can induce permanent growth arrest in primary cell types (3). This cell fate program indeed occurs in response also to environmental stresses, mainly oxidative stress (SIPS: stress-induced premature senescence) (4), and activated oncogenes (OIS: oncogene-induced senescence) (5). Compelling evidences obtained in recent years demonstrate that DNA damage is a common mediator for both replicative senescence triggered by telomere shortening and premature senescence induced by oncogenic stress, oxidative stress and others stressors.

A key concept is that senescent cells have common evident features despite the multiple cellular types involved. These features are termed

"biomarkers" (Figure 1) (6). The most obvious biomarker is the growth arrest, which can be detected by analysis of levels of cell-cycle related

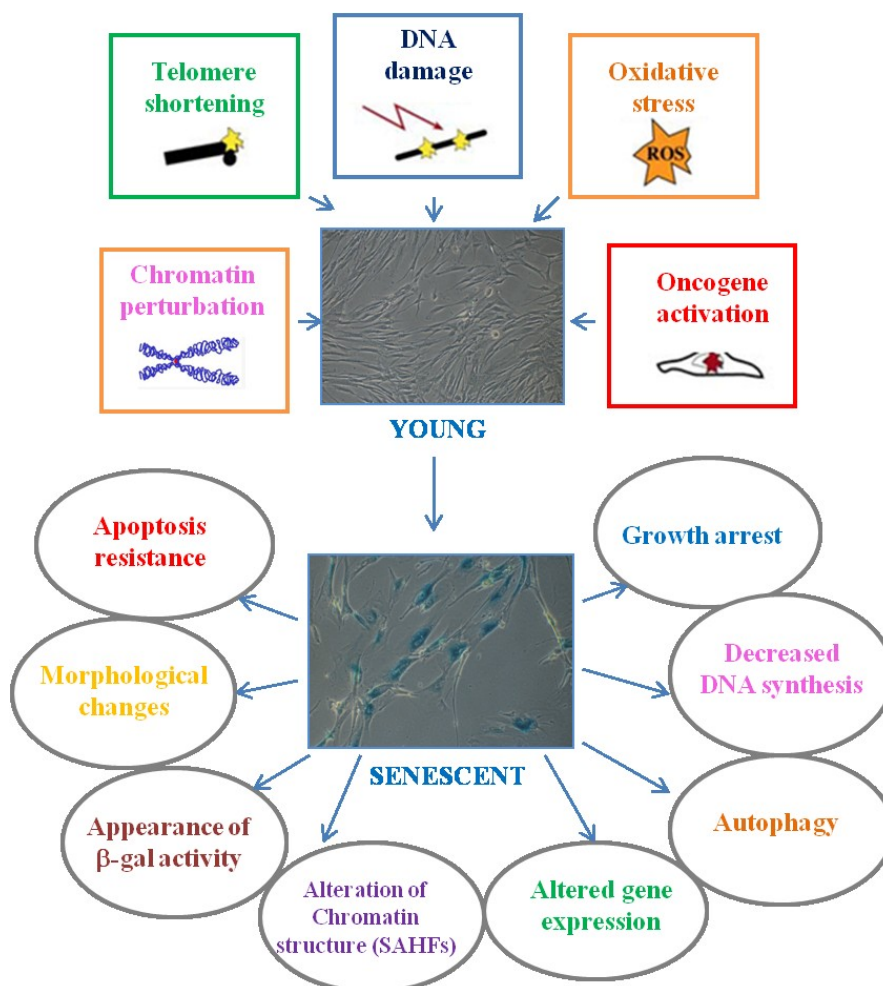


Figure 1: Causes of senescence and main features of senescent cells. The major cause of senescence is critically short telomeres but this is only one of signals that can induce permanent growth arrest in primary cell types. This cell fate program occurs in response also to environmental stresses, mainly oxidative stress, activated oncogenes, DNA damage and other stimuli.

All forms of cellular senescence share common features: growth arrest, morphological changes, decreased synthesis of DNA, modification of gene expression profiles, altered response to apoptosis, increased β -galactosidase activity and alteration of chromatin structure with appearance of specific foci called senescence-associated heterochromatic foci (SAHFs).

proteins and DNA synthesis. In fact, various cell growth-regulatory proteins, including p21^{WAF1}, p16^{INK4a} are up-regulated with senescence and exhibit altered activation states. Another important biomarker is the cellular morphology. The progressive morphological changes were particularly well-studied by Klaus Bayreuther and colleagues (7). In brief, senescent cells become flattened, enlarged, granular and lacking vacuoles. Furthermore, senescent population has more diverse morphologies than young cells. In fact, a confluent senescent culture has a smaller cellular density than a confluent one, though this also occurs because senescent cells are more sensitive to cell-cell contact inhibition. In 1995, Judith Campisi and her team discovered that the enzyme β -galactosidase, a lysosomal hydrolase, has an abnormal behavior in senescent cells. This activity was termed senescence-associated β -galactosidase (SA- β -galactosidase). While the significance of this change is still not clear, it appears to result from rather profound changes in the lysosomal compartment of senescent cells. This lysosomal enzyme is normally active at pH 4, but its quantity increases to a level that can be detected at suboptimal pHs, such as 6.0 (8). Both *in vitro* and *in vivo*, the percentage of positive cells for SA- β -galactosidase increases with, respectively, population doubling level (PDL) and age (9). In many cell types, such as human fibroblasts, senescence arrest is accompanied by formation of distinct structures, referred to as senescence-associated heterochromatic foci (SAHF), that accumulate in the cellular nuclei and silence proliferation-promoting genes, such as cyclin A. SAHF positive cells have been shown to occur with the same kinetics as other markers of senescence (SA- β -galactosidase, p21^{WAF1} and p16^{INK4a} over-expression). Moreover, during senescence, SAHFs strongly correlate with the irreversibility of the senescent phenotype and might be the mechanism that defines the point of no return in terms of growth arrest (10). As mentioned before, DNA damage is a common mediator of the onset of cellular senescence. The relevance of DNA damage response (DDR) in the induction of permanent growth arrest is highlighted by the observation that hallmarks of DDR, known as senescence-associated DNA-damage foci (SDFs) can be identified in aging mammalian tissues. Also senescent human fibroblasts display molecular markers characteristic of cells bearing DNA double-strand breaks. These markers include nuclear foci of phosphorylated histone H2AX and their colocalization with DNA repair and DNA damage checkpoint factors such as 53BP1, MDC1 and NBS1 (see after). Senescent cells show striking changes in gene expression. Various growth-regulatory genes exhibit altered expression; in fact they are

upregulated in senescence and are involved in cell-cycle arrest. Senescent cells also repress genes that encode proteins that stimulate or facilitate cell-cycle progression. Interestingly, many changes in gene expression appear to be unrelated to the growth arrest. Many senescent cells overexpress genes that encode secreted proteins. In fact, senescent cells also display the capacity to communicate with their environment by secreting a myriad of factors. This “senescence associated secretory phenotype (SASP), also known as “senescence messaging secretome” (SMS), includes a wide range of growth factors, proteases, chemokines and cytokines of the proinflammatory networks, such as IL-6 and IL-8, which could have many paracrine effects on the extracellular environment (11).

Like senescence, apoptosis is an extreme response to cellular stress and is an important tumor-suppressive mechanism. But, whereas senescence prevents the growth of damaged or stressed cells, apoptosis quickly eliminates them. Many (but not all) cell types acquire resistance to certain apoptotic signals when they become senescent and this phenomenon might partly explain why senescent cells are so stable in culture (12). It is not clear what determines whether cells undergo senescence or apoptosis. One determinant is cell type; for example, damaged fibroblasts and epithelial cells tend to senesce, whereas damaged lymphocytes tend to undergo apoptosis. The nature and intensity of the damage or stress may also be important (13). Moreover, manipulation of pro- and anti-apoptotic proteins can cause cells that are destined to die by apoptosis to senesce and, conversely, cause cells that are destined to senesce to undergo apoptosis (14). The senescence and apoptosis regulatory systems therefore communicate probably through their common regulator, the p53 tumor suppressor protein (15). The mechanisms by which senescent cells resist apoptosis are poorly understood. In some cells, resistance might be due to expression changes in proteins that inhibit, promote or implement apoptotic cell death. In others, p53 might preferentially transactivate genes that arrest proliferation, rather than those that facilitate apoptosis (16). Other results also suggest that during *in vitro* aging increased autophagy. Autophagy is a genetically regulated program responsible for the turnover of cellular proteins and damaged or superfluous organelles. Autophagy is often associated with acute metabolic changes and rapid protein replacement. It is identified that autophagy as a new effector mechanism of senescence, important for the rapid protein remodeling required to make the efficient transition from a proliferative to a senescent state (17). Cellular senescence is thought to have evolved as a mechanism to prevent

damaged DNA being passed on to future generations of cells and for this reason it can be considered a tumor suppressor mechanism. In fact, a series of studies have reported that senescent cells are abundant within pre-malignant neoplastic lesions, but scarce in malignant tumors (18). Numerous evidences support the hypothesis that cellular senescence *in vivo* exerts a critical role in organism aging and aging-associated degenerative diseases. It is now widely accepted that the progressive accumulation of senescent cells with age, leads to decline in tissue homeostasis, most likely through stem cell depletion and/or tissue structure impairment/disruption (19). At the same time, the persistence of senescent cells entails an increased expression of SASP factors that contribute to chronic inflammation which drives aging and most age-related diseases (19). Thus, senescence can be considered a double-edged sword: on one hand can be viewed as a mechanism of defence to neoplastic transformation; on the other hand, with the abnormal paracrine signalling, could contribute, *in vivo*, to the general and progressive deterioration recognized as *in vivo* aging, thereby promoting age-related diseases (20).

1.2 Molecular mechanisms of cellular senescence.

Detailed investigations at the molecular level have revealed two major tumor suppressor pathways for the induction of cellular senescence: p53/p21^{WAF1} and p16^{INK4a}/Rb (Figure 2). Replicative senescence is telomere-dependent and is mediated by the p53- p21^{WAF1} pathway (20) and also encompasses the DNA-damage response (DDR) mechanism. In contrast, a telomere-independent mechanism of senescence, typically activated by oxidative stress, is mediated by the p16^{INK4a} pathway (21, 22). Both of these pathways converge on retinoblastoma protein (Rb), which is responsible for allowing progression from G1 to S phase.

1.2.1 p53 pathway

A linear sequence of events has been elucidated involving the transcriptional activator and tumor-suppressor protein, p53; the cyclin-dependent kinase inhibitor, p21^{WAF1} and the cell-cycle regulator, Rb, as the principal players in telomere-dependent senescence.

p53 has been named the “guardian of the genome” and is mutated in 50% of all tumors. It acts as an integrator for various signal stresses and can mediate cell cycle arrest, DNA repair, apoptosis, senescence and differentiation. The type of response is affected by cell type, oncogenic status, intensity of stress and p53 expression level. The sensing of DNA damage, including telomere shortening, and activation of p53 in G1

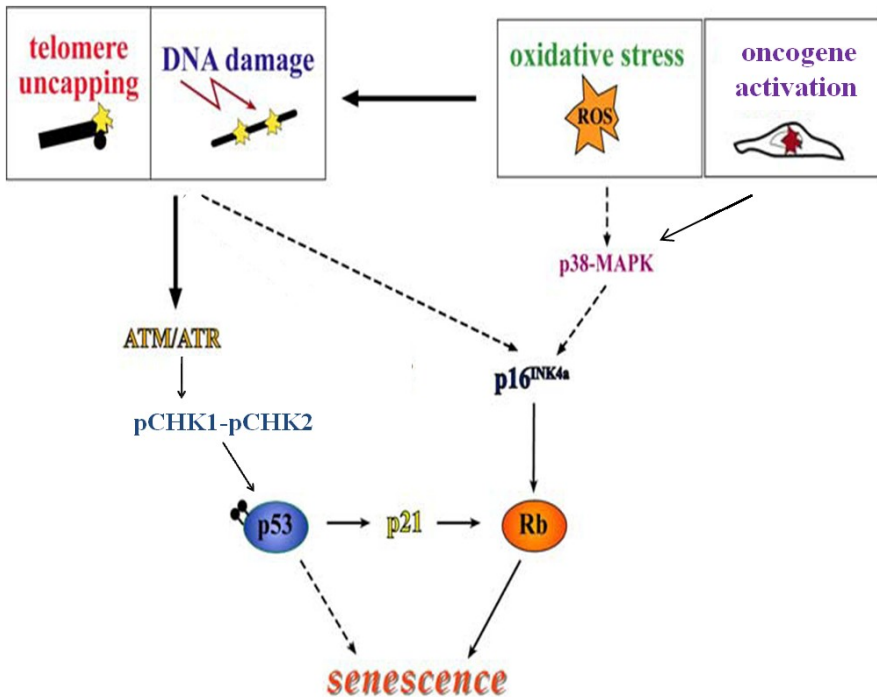


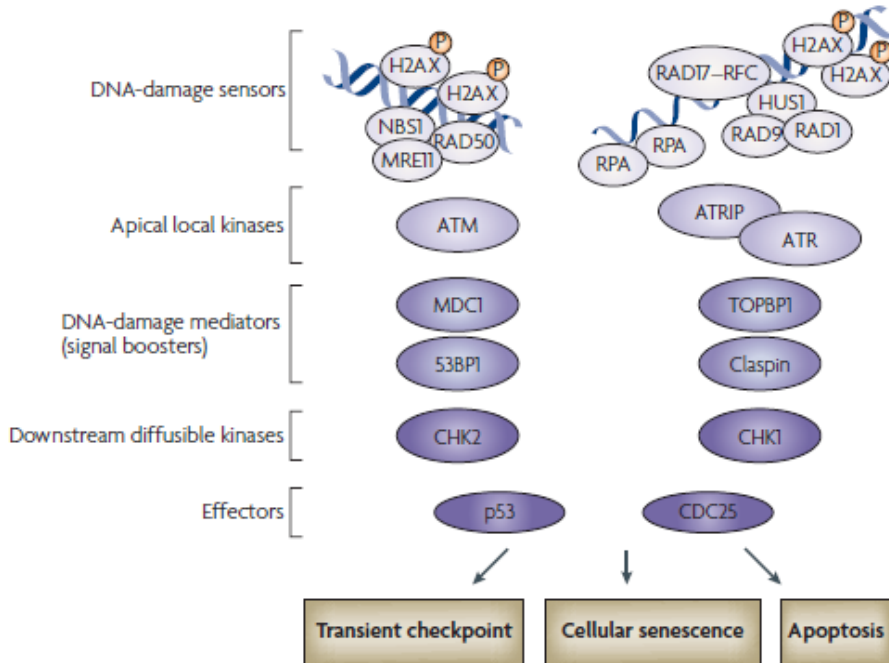
Figure 2: Signaling pathways leading to cellular senescence.

The onset of cellular senescence is regulated by two tumor-suppressor pathways, p53-p21^{WAF1}-Rb and p16^{INK4a}-Rb. Telomere shortening induces senescence mainly through the DNA damage pathway, activating the ATM/ATR pathway and CHK1/CHK2 to stabilize p53. In human cells p16^{INK4a} is activated in certain settings in response to telomere shortening, through unknown pathways. Direct DNA damage activates the senescence program mainly through p53, in essentially the same manner as telomere shortening.

Oxidative stress induces DNA damage, and also accelerates telomere shortening, possibly leading to accelerated telomere uncapping. The downstream response is mediated through the DNA damage pathway and through activation of p16^{INK4a}, and may be mediated through p38MAPkinase. RAS oncogene activation induces senescence mainly through p16^{INK4a} in human cells. p38MAPkinase plays a role in mediating RAS-induced senescence. p16^{INK4a} is also activated by additional physiologic stresses, such as nutrient and growth factor deficiency. The exact stimuli for this activation and the pathways mediating it are unknown.

prevents abnormal DNA being replicated in S phase. The functions of cell-growth arrest and apoptosis are therefore critical roles of the p53 protein: it limits the ability of damaged cells to pass on aberrant DNA or to develop neoplastic potential. Indeed, many human tumors possess mutated p53 protein that is deficient in activity (23, 24, 25), whereas suppression of p53 expression results in emergence of cells from senescence, resumption of replication and immortalization (26). Initial evidence for the transcriptional regulation of p53 during replicative senescence was provided by Kulju and Lehman (27), who found p53 mRNA and p53 protein levels increased in senescent IMR-90 diploid fibroblast compared with young cells. They also noted an increase in phosphorylated p53 in cells nearing senescence. The mechanisms by which telomere-shortening or DNA-damage signals are transduced to the p53 protein remain to be fully elucidated. Double strand breaks (DSBs) are sensed by specialized complexes (MRN), formed by MRE11, Rad50, NBS1 that recruit and activate two large protein kinases, ataxia telangiectasia and Rad3-related (ATR) or ataxia-telangiectasia mutated (ATM), respectively, at the site of the DNA lesion. ATM undergoes auto-phosphorylation and activated ATM phosphorylates the histone variant H2AX. By a complex action of sensors, transducers and effectors, ATM and also ATR induce p53 phosphorylation (28). ATM and ATR translocate to sites of DNA damage where the histone H2AX is phosphorylated to γ -H2AX (in fact this is used such as marker of senescence). γ -H2AX is thought to induce changes in the local chromatin structure, thus facilitating in the focal assembly of DNA-repair proteins and the checkpoint proteins CHK1 and CHK2. ATM and ATR are then able to phosphorylate CHK1 and CHK2, which subsequently activate p53 (29, 30, 31, 32). ATM can phosphorylate p53 directly or indirectly by phosphorylation of CHK2 at Thr68 (33), which in turn directly phosphorylates p53 (34, 35) (Figure 3). Because of the critical role that p53 has in controlling cellular activities, the mechanisms regulating p53 are necessarily complex and consist of a range of post-translational changes to the protein. These include phosphorylation (36), acetylation (37) and redox control (38). Once activated, p53 initiates a series of downstream transcriptional events. An immediate target is the p21 gene (39), which encodes the potent cyclin-dependent kinase 2 (Cdk2) inhibitor, p21^{WAF1}. In fact, p21^{WAF1} is overexpressed in senescent cells (39), that generally arrests cell-growth in G1 phase. The downstream target of p53, p21^{WAF1} can induce senescence in tumor cell lines independent of p53 status (40), and human diploid fibroblasts lacking p21^{WAF1} bypass senescence (41)

This indicates an important role of p21^{WAF1} for induction of senescence in human cells.



From D'Adda di Fagagna, *Nature Review Cancer*, 8: 512-522 (2008).

Figure 3: The DNA -damage response (DDR).

The DDR is robustly activated by double strand breaks (DSBs) and/or the exposure of single-stranded DNA (ssDNA). DSBs are sensed by the MRE11–RAD50–NBS1 (MRN) complex and NBS1 recruits the apical protein kinase ATM. ATM undergoes autophosphorylation, and activated ATM phosphorylates the histone H2A variant H2AX at the site of DNA damage. γ H2AX (phosphorylated H2AX) is recognized by a phospho-specific domain of MDC1, that fuels the additional accumulation of MRN (to which MDC1 binds), which leads to amplified local ATM activity and the spreading of γ H2AX along the chromatin. This in turn causes a local increase of several DDR factors at the site of DNA damage, thereby generating a positive feedback loop that amplifies ATM activity.

Single-stranded DNA is sensed by the protein RPA (replication protein A) that localized at sites of SSD. Once RPA-coated single-stranded DNA forms, the recruitment of the heterodimeric complex that comprises ATR (a paralogue of ATM) and its DNA-binding subunit ATRIP is favored.

Not all DDR factors accumulate at sites of DNA damage. The protein kinase CHK2 is thought to transiently localize at sites of DNA damage only for enough time to be phosphorylated and activated by ATM. Similarly, although a fraction of CHK1 is chromatin bound in undamaged cells, ATR-dependent phosphorylation of CHK1 allows it to freely diffuse in the nucleus. Therefore, both CHK1 and CHK2 are responsible for DDR signalling in nuclear regions distant from the DNA-damage site. Finally, p53 induces cell-cycle arrest by activating the transcription of p21^{WAF1}, a CDK inhibitor that blocks cell-cycle progression.

Rb is a cell-cycle regulator, one function of which is to control progression from G0 and G1 to S phase (42). Cell-cycle progression is dependent on hyperphosphorylation of Rb by cyclin-dependent kinases in association with cyclins to allow transcription of proliferative genes. Rb is regulated by Cdk2, Cdk4, and Cdk6 phosphorylation. p21^{WAF1} and p16^{INK4a} are Cdk inhibitors thereby leading to Rb hypophosphorylated. Hypophosphorylation of Rb inactivates the E2F transcription factor required for progression through S phase (43). The level of phosphorylation of Rb is fundamental to the correct regulation of its activities: the hyperphosphorylated form (active) predominates in proliferating cells, while hypophosphorylated (inactive) predominates in senescent cells (44).

1.2.2 The p16^{INK4a} pathway

p16^{INK4a} is a critical regulator of cellular senescence acting through Rb but independent of p53 (Figure 2). Many senescence triggers have been shown to upregulate p16^{INK4a}, including activated oncogenes, DNA damage, ROS, oxidative stress, dysfunctional telomeres and other poorly defined cell stresses (45). However, p16^{INK4a} is not as acutely or specifically responsive to DNA damage and dysfunctional telomeres as is the p53 target, p21^{WAF1}. The expression of p16^{INK4a} is found to be increased in some senescent human fibroblasts, but several lines of evidence indicate that p16^{INK4a} induction is unlikely related to telomere shortening. The increased expression of p16^{INK4a} occurs after senescence has already been established in culture (46), in contrast to the rapid increase of p21^{WAF1} expression in cells approaching replicative senescence (47). Recent studies have revealed that a senescent population of human cells in culture is a mosaic of distinct subpopulations, some of which express p16^{INK4a}, while others express p21^{WAF1} (48). p16^{INK4a} is responsive to more diverse stresses, through distinct regulatory pathways. Two of the best characterized of these are polycomb group complexes (PcGs) and stress-activated kinases p38MAPkinases. Several studies have implicated PcGs as direct regulators of the CDKN2a gene, which codes for p16^{INK4a} and alternative reading frame (ARF), an indirect activator of p53 (45). PcGs are collaborating multisubunit transcriptional repressor complexes that are direct repressors of p16^{INK4a} expression in proliferating cells, and their inactivation in senescent cells contributes to upregulation of p16^{INK4a}. Several other studies have established that the stress-activated p38MAPkinases contribute to senescence-associated upregulation of p16^{INK4a} (49). Like p16^{INK4a}, p38MAPkinase is activated by diverse stresses, including short telomeres, ROS and activated oncogenes. Between these triggers and activation of p38MAPkinase there

are various effectors, including MKK3/6 kinases in response to chronic RAS/ERK activation and the ROS activated MINK kinase.

The mechanism by which p38MAPkinases activates p16^{INK4a} is not clear. Since one target of p38MAPkinase is the kinase MAPKAPK3, which has been reported to phosphorylate PcG proteins (50). It is possible that p38MAPkinase acts through PcGs. Phosphorylated PcGs dissociate from chromatin and derepress CDKN2A (50). In sum, p38MAPkinases and PcG proteins contribute to a stress-p38MAPkinase-PcG-p16^{INK4a} pathway that is activated by diverse triggers of senescence

1.3 Causes of senescence

Most somatic cells have a finite number of divisions and eventually become senescent because of telomere shortening. In addition to replicative senescence, a senescent phenotype can be induced prematurely in early passage cells by several factors such as oxidative stress, overexpression of oncogenes, disruption of heterochromatin and in general by stressors that can elicit a DNA damage response. These forms of premature senescence are typically induced within several days and are not normally accompanied by telomere shortening.

1.3.1 Telomere dysfunction

The onset of replicative senescence is determined by the number of times that a cell population divides, suggesting that a mitotic clock records cell divisions (51, 52). It is now known that this clock is calibrated by telomere shortening in mammals (53, 54). Telomeres are guanine rich DNA regions composed of repetitive sequences (5'-TTAGGG-3'), that associate proteins to cap the ends of chromosomes. Telomeres have the critical function of protecting the end of linear chromosomes that short at each round of DNA replication. For each population doubling, telomeres tend to lose approximately 100 base pairs and when their length is drastically reduced the cells enter senescence assuring a finite number of replications. Experimental data suggest that the cellular life span can be measured by the progressive loss of telomere repeats and that silent genes adjacent to telomeres mediate senescence initiation (55). The critical length of telomeres is less than 5 kb and represents the threshold at which p53 and Rb pathways are activated and trigger senescence (56). The activity of the enzyme telomerase maintains the length of telomeres in germ cells and stem cells but not in most somatic cells in which this enzyme is not active. As a result, the length of telomeres gradually decreases during each replication. As mentioned before, the progressive shortening of telomeres is connected to the process of organismal aging

and to the activation of cellular senescence. By restoring and maintaining the telomere length, telomerase is believed to act as a “molecular clock” that functions to regulate the replication activity of cells and the onset of senescence (57). A strong telomerase activity has been detected in immortalized and tumor cells leading to the capacity to replicate infinitely and to a possible loss or inactivation of expression of specific genes involved in the senescence program and regulation of the normal cell cycle (58). The limited number of cell replications guaranteed by the gradual shortening of telomeres might protect the organism from the occurrence of cancer. Loss or dysfunction of telomeres indeed might lead to genomic instability and DNA damage. Therefore, the onset of senescence as a response to short dysfunctional telomeres represents a mechanism of tumor suppression *in vivo* that arrests division and growth of damaged cells at risk of malignant transformation (59). The mechanisms by which shortened telomeres are sensed and the senescence program is activated remain elusive. It has been proposed that telomere shortening acts as signal of DNA damage checkpoint pathway. The dysfunction detected in short telomeres activates a response similar to the one activated by DSBs (60) and activation of ordinarily silent “senescence genes” located in SAHF (61).

Recently, markers for DNA damage response, such as nuclear foci of phosphorylated histone H2AX, 53BP1, and MRE11 have been observed to localize at telomeres in senescent cells after serial passage (60), indicating that DNA damage response can be triggered by telomere shortening.

1.3.2 Oxidative stress.

Since Harman proposed the “free radical theory of aging”, oxidative stress is considered the major cause of cellular senescence and the aging of organism. According to this theory, the accumulation of oxidative damages produced by ROS at DNA, proteins and lipids results in loss of cellular homeostasis with accumulation of senescent cells and consequently aging (62). ROS are defined as compounds with high chemical reactivity due to an unpaired electron in the external orbital. The most important in biological functions are: superoxide anion ($O_2^{\bullet-}$) and nitric oxide (NO^{\bullet}). Other molecules, such as H_2O_2 (hydrogen peroxide) are not radicals itself but they easily produce, in the presence of iron, hydroxyl radical ($\bullet OH$), particularly harmful and difficult to control (63, 64). In biological systems, ROS are constantly generated and eliminated. Cells, in fact, maintain an intracellular reducing environment and this redox state is insured by a normal intracellular balance between

ROS production, oxidant, and antioxidant defense systems (activities "scavengers" or "scavenger") of enzymatic nature, such as glutathione peroxidase complex and superoxide dismutase mitochondrial (SOD) and non-enzymatic compounds such as vitamins A, C, E, and polyphenols. The superoxide anion is neutralized by SOD enzyme that converts $O_2^{\bullet-}$ in H_2O_2 . The cells therefore have developed a sophisticated system of defense against ROS. All work as scavengers of ROS, but can not directly intervene on biological macromolecules to remove the damage when it has already happened (65). Oxidative stress occurs when the amount of ROS overwhelms the reductive capacity of SOD and other protective systems. Harman's theory on ROS as a cause of aging has not yet been demonstrated in vivo, despite recent data obtained mainly in *Caenorhabditis elegans*, *Drosophila* and in mouse show a positive correlation between increased resistance to oxidative stress and elongation of life span (66, 67). On the contrary, the correlation between oxidative stress and senescence in vitro is well documented and numerous literature data have shown that natural oxidant compounds induce premature senescence. In fact, human fibroblasts undergo premature senescence when grown in high ambient oxygen conditions, 40–50% oxygen. Conversely, the proliferative lifespan of these cells is extended when they are grown in low ambient oxygen, 2–3%, a condition more closely resembling physiologic oxygen levels (68, 69). Similarly, increase of intracellular ROS levels through hydrogen peroxide treatment or through the inhibition of ROS scavenging enzymes, such as superoxide dismutase SOD1, causes premature senescence (70). The activity of proteasome complex, that degrades oxidized proteins, has been observed to decline during senescence suggesting that oxidative stress induces accumulation of oxidative proteins that cannot be efficiently degraded. It has been suggested that oxidative stress, like telomere dysfunction, could acts through the $p53 \rightarrow p21^{WAF1} \rightarrow Rb$ axis to induce senescence. Other studies indicate, however, that $p16^{INK4}$ can be also activated in response to oxidative stress, possibly through the action of the p38MAPkinase protein (71).

1.3.3 **DNA-damage induced by drugs.**

The direct damaging of DNA achieved by treatment with DNA damaging agents, such as etoposide, cisplatin can induce cells to undergo senescence. Often though, the cellular response to several damages is cell death or reversible cell-cycle arrest, depending on the type of agent, the dosage administered and the type of cell treated (72).

Treatment of human fibroblasts with cytotoxic chemotherapeutic agents generally induces apoptosis or senescence in a dose-dependent manner. Treatment with low doses induces premature senescence whereas higher doses induce apoptosis. Etoposide in vitro reduces proliferation by inducing an irreversible arrest of cell cycle before mitosis, resulting in accumulation of cells in S and G2 phase of cell cycle. This effect is typical of drugs that interfere with DNA, affecting breaking one or both strands. It is known that the cytotoxic action of etoposide is dependent on its action on topoisomerase II. This enzyme plays a key role in the maintenance of physiological function allowing the breakage and repair of DNA during synthesis. In presence of etoposide, the enzyme forms a stable complex with DNA and this complex prevents the reunification with the rest of the DNA double helix. This event causes single and double-strand breaks, which inhibit DNA synthesis in the terminal phase. Treatment of human fibroblasts with low doses of etoposide (20 μ M) for a short period of time induces a DNA damage quickly highlighted and a massive induction of senescence after few days of treatment (73).

1.3.4 Oncogene-induced senescence (OIS)

Oncogene activation is a hallmark of cell transformation and cancer. However, oncogene activation in a normal cell does not lead to cell transformation, but instead induces cellular senescence (74). This paradox can be explained by considering the level of oncogene activation: low levels of oncogenes are involved in the onset of cancer while high levels are causative of the senescent phenotype. OIS is therefore a tumor suppressive mechanism that impedes the proliferation of a cell that expresses high levels of an aggressive oncogene. Importantly, this type of senescence is established independently of any telomere attrition or dysfunction (75). OIS was induced by several oncogenes, such as H-RAS^{G12V}, BRAF^{E600}, E2F1, MYC. It has recently been observed that cellular senescence, which is mediated by many different oncogenes and signalling factors, is associated with DDR activation (76, 77). Indeed, aberrant activation of signal transduction pathways and positive cell-cycle regulators can lead to the accumulation of DNA damage, full engagement of the DDR cascade and appearance of SDFs. Time-course studies have revealed that expression of the oncogenic form of HRAS leads to a biphasic response (78). RAS drives an initial hyperproliferation phase in which cells proliferate faster than control cells. However, this burst of proliferation is transient and is quickly followed by a proliferation slow down and the eventual establishment of cellular senescence (77). This biphasic response has also been observed following the expression of other oncogenes, such as

BRAF, *E2F1* and *MYC* (77, 78, 79). DDR activation coincides in time with the end of hyperproliferation and entry into senescence. Interestingly, the engagement of the DDR pathways is subtly different in telomere attrition-induced and OIS. Telomere attrition mainly triggers ATM activation, with ATR engagement being detectable only in the absence of ATM. Conversely, ATR, have been detected in response to OIS (80).

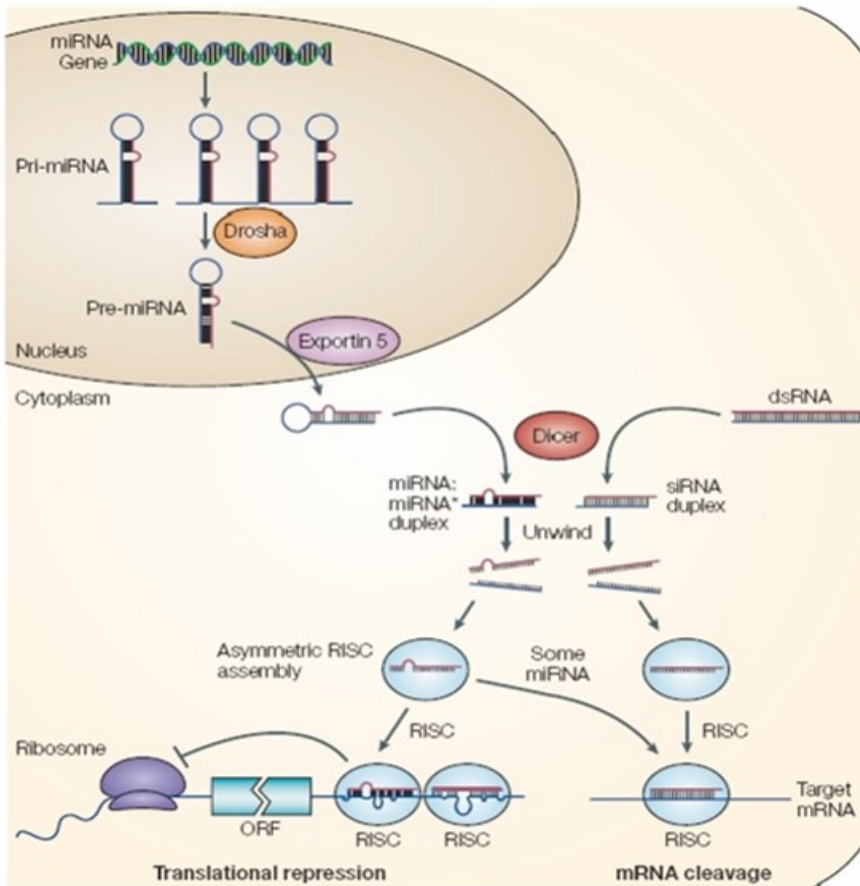
Although much remains to be learned about the mechanisms that lead to DNA-damage generation and DDR activation following oncogene activation, oncogene-induced DDR activation and senescence have been proposed to result from altered DNA replication. The best evidence that links an oncogene to DNA replication regulation is the recent discovery that *MYC* binds to DNA replication origins and activates the replication machinery. However, this is associated with the accumulation of DNA damage and activation of a DDR (79). Furthermore, oncogenic *HRAS* expression impacts on DNA replication and increases the number of simultaneously active DNA replication origins. This suggests that increased DNA-replication-origin usage caused by oncogenic depletes limiting DNA replication factors or generates regions of single-stranded DNA, which activate the ATR-dependent checkpoint (76). Thus, together with the observation that activated DDR markers localize at sites of ongoing DNA replication in oncogene-expressing cells, indicate that oncogene-induced DDR activation is a strictly DNA-replication-dependent event.

1.4 MicroRNAs

The recent identification of microRNAs (miRNAs, miRs) has added a new layer of complexity to the regulation of gene expression. microRNAs are non-coding single-strand RNAs (ssRNAs) of ~22 nt in length in their mature forms. They normally function as negative regulators of target mRNA expression at post-transcriptional level. microRNAs bind to the 3'UTR of target mRNAs through base pairing, resulting in target mRNA cleavage or translation inhibition. It is believed that about 60% of human protein coding genes are regulated by microRNAs. Genes for microRNAs are an integral component of the cell genetic program, many of them also being evolutionarily conserved (81). The discovery of microRNAs was made in 1993, when Lee, Feinbaum, and Ambros discovered that *lin-4*, a gene of *Caenorhabditis elegans* did not code for a protein but instead produced a pair of short RNA transcripts that regulate the timing of larval development by translational

repression of *lin-14*, which encodes for a nuclear protein (82). They postulated that the regulation was due in part to sequence complementarity between *lin-4* and unique repeats within the 3' UTR of the *lin-14* mRNA. The downregulation of *lin-14* at the end of the first larval stage initiates the developmental progression into the second larval stage. (83). It was 7 years later that the second microRNA, *let-7*, was discovered (84). Since the discovery of *let-7*, thousands of microRNAs have been identified in organisms as diverse as viruses, plants, worms, and primates through random cloning and sequencing or computational prediction (85, 86). The identified microRNAs are currently curated and annotated at miRBase, hosted by the Sanger Institute as an available repository.

Studies on microRNA gene distribution throughout the genome have revealed their presence in clusters transcribed as polycistronic primary transcripts, or within regions transcribed as independent units, including intergenic regions, exon sequences of non-coding transcription units or intronic sequences of either protein coding or non-coding transcription units (87, 88). Intronic microRNAs orientated in the same direction of the surrounding genes are generally transcribed coincidentally with their host genes and excised by the splicing machinery from the larger transcript in which they are embedded (81). The biogenesis of microRNAs is illustrated by Figure 4.



From He et al., *Nature Reviews Genetics*, 5: 522 (2004)

Figure 4: Biogenesis of microRNAs.

microRNA genes are transcribed generally by RNA polymerase II (Pol II), generating the primary miRNA (pri-miRNA). In the nucleus, the RNase III endonuclease Drosha and the double-stranded RNA-binding domain (dsRBD) protein DGCR8/Pasha cleave the pri-miRNA to produce a 2-nt 3' overhang containing the ~70-nt precursor miRNA (pre-miRNA). Exportin-5 transports the pre-miRNA into the cytoplasm, where it is cleaved by another RNase III endonuclease, Dicer, together with the dsRBD protein TRBP/Loquacious, releases the 2-nt 3' overhang containing a ~21-nt miRNA:miRNA* duplex. The miRNA strand is loaded into an Argonaute-containing RNA-induced silencing complex (RISC), whereas the miRNA* strand is typically degraded. Once incorporated into RISC, the microRNA guides the complex to mRNA targets by base-pairing interactions. In cases of perfect or near-perfect complementarity to the microRNA, target mRNAs can be cleaved (sliced) and degraded; otherwise, their translation is repressed.

Transcription of microRNAs is typically performed by RNA polymerase II (Pol II). Primary transcripts, called pri-miRNAs, may be several kilobases long, bearing hairpin-shaped structures and transiently receive a 5' cap and a poly(A) tail similar to that of the mRNAs. Recent studies, however, have shown that the RNA Pol III drives microRNA transcription from dense human clusters interspersed among repetitive Alu elements (89).

The pri-miRNA is processed within the nucleus by a multiprotein complex called the Microprocessor, the core components of which are the RNase III enzyme Drosha and the double-stranded RNA-binding domain (dsRBD) protein DiGeorge syndrome chromosomal region 8 (DGCR8/Pasha) (90, 91). This complex cleaves the pri-miRNA producing a 70-nt hairpin precursor microRNA (pre-miRNA). The 2-nt 3' overhang, characteristic of RNase III-mediated cleavage, is recognized by Exportin-5, which transports the pre-miRNA into the cytoplasm via a Ran-GTP-dependent mechanism (92, 93). Next, the pre-miRNA is cleaved to produce a mature 22-nt miRNA:miRNA* duplex by another RNase III enzyme, Dicer. This enzyme together with TRBP and Argonaute protein 2 (Ago2) forms a trimeric complex that initiates the assembly of the RNA-induced silencing complex (RISC), a ribonucleoprotein complex capable of binding dsRNA (94, 95). The microRNA strand with relatively lower stability of base-pairing at its 5' end is incorporated into RISC (miRISC complex), whereas the microRNA* strand is typically degraded (96). Once incorporated into RISC, the microRNA guides the complex to mRNA targets by base-pairing interactions. In cases of perfect or near-perfect complementarity to the microRNA, target mRNAs can be cleaved (sliced) and degraded; otherwise, their translation is repressed (97, 98). Most animal microRNAs base-pair imperfectly with their targets and promote translational repression rather than cleavage and degradation. The mechanism of translational repression by microRNAs remains unclear. Indeed, the step at which microRNAs block translation is controversial. There is evidence that microRNAs block translation initiation, whereas other studies suggest a block in elongation (99, 100, 101, 102,).

Therefore, the mechanisms proposed are three:

1. miRISC mediates repression of translation because Ago2 itself competes with eIF4E for cap binding;
2. miRISC stimulates deadenylation of the mRNA tail;
3. miRISC block association of ribosomal subunits.

Another important issue about microRNA-mediated regulation is the localization within cells of miRISC complex. Argonaute proteins and

microRNAs and their target mRNAs accumulate in processing bodies (P-bodies), cytoplasmic foci that are known sites of mRNA degradation (102, 103). P-bodies exclude ribosomal components and may therefore serve as sites in which mRNAs can be stored without translation. Several proteins found in P-bodies can bind to Argonaute proteins, and this interaction mediates translational repression (104, 105). Yet, doubts remain over the importance of P-bodies in target repression. Disrupting P-bodies does not affect the degree of translational repression, and therefore the P-body localization may be a consequence of repression rather than its cause (106). Moreover, microRNA-mediated repression and P-body localization are reversible (107), indicating that the P-bodies may serve as sites of temporary storage of translationally repressed mRNAs. Due to multiple targets of each single microRNA, which are estimated several hundreds, they might resemble transcription factors that influence numerous cellular responses. In fact, microRNAs are involved as prominent regulators or fine-tuners in virtually all regulatory gene network, concerning development, cell proliferation, apoptosis and cancer.

1.5 Biological role of microRNA in senescence

In low organisms as *Caenorhabditis elegans* the microRNA lin-4 has been associated with life expectancy and mutations in gene greatly affects the lifespan of *Caenorhabditis elegans* (108). In more complex organisms a only few numbers of microRNAs have been linked to cellular senescence. Overwhelming evidences of the involvement of microRNAs in cellular senescence arise from the effect of Dicer's knock-out, that resulted in premature senescence of mouse embryonic fibroblasts (MEFs). Ablation of Dicer, with the consequent loss of mature microRNAs, resulted in increased DNA damage, and p53 levels that lead to inhibition of cell proliferation and premature senescence (109). This evidence indicates that alteration of microRNA levels is strongly correlated to induction of senescence. The contribution of microRNAs to the induction and maintenance of the senescent phenotype might involve the regulation of different cellular pathways. The most investigated is influencing the cell cycle progression. In this regard many studies show that the let-7 family of microRNAs inhibits KRAS and c-MYC, related to cell cycle. Similarly, microRNAs 15a/16-1 cluster and the microRNA-17-92 cluster are potent regulators of cell cycle progression by targeting Cdk6 as well as the Cdk inhibitor family members p21^{WAF1}, p27 and p57 as reviewed recently (110). Another

example is microRNA 34, which is under the control of p53 (111). This microRNA functions as a tumor suppressor and its overexpression in fibroblasts IMR90 induces a senescent phenotype. In murine fibroblasts MEF, microRNA 20 induces a senescent phenotype through upregulation of p16^{INK4a} (112).

microRNAs might also be involved in the perturbation of the microenvironment surrounding the aged cells, by modulating secretion of proteins like extracellular matrix or cytokines. In regard to secretion of cytokines, it is of note that microRNA-146a/b, which are upregulated in senescent fibroblasts, are inhibitors of IL-6 and thus might contribute to the protein secretion alterations observed in senescent cells (113).

1.6 Scientific hypothesis and aim of the work

The aim of this work was to evaluate the role of the microRNAs in the cellular senescence, in particular in the induction of senescence in human primary fibroblasts IMR90. Cellular senescence is now recognized as a mechanism to prevent tumorigenesis and a possible contributor to aging. microRNAs are regulators of gene expression at post-transcriptional level. Emerging evidences indicate a crucial role of microRNAs in the induction and maintenance of senescent phenotype. The purpose of the present investigation is:

- To analyze the differential expression of microRNAs in senescent (late passages) relative to young human diploid fibroblasts IMR90 (early-passage);
- To validate these expression data in another example of replicative senescence in normal BJ cells and in premature senescence of IMR90, induced with diethylmaleate (DEM) compound, able to induce oxidative stress and with Etoposide, a DNA damaging agent;
- To analyze the effects of the manipulations of selected upregulated microRNAs in young IMR90 to investigate whether the variations of intracellular levels of some microRNAs is a causative event of senescence;
- To explore molecular mechanisms by which selected microRNAs are involved in the onset of the senescence, in particular by focusing on the pathway of the DNA damage response (DDR).

2. MATERIALS AND METHODS

2.1 Cell cultures and replicative senescence.

IMR90 cells, human primary fibroblasts (ATCC, population doubling level -PDL- 25) and BJ cells, human neonatal foreskin (ATCC, PDL 24) were cultured in Dulbecco's modified Eagle's medium (Gibco) supplemented with 10% (v/v) fetal bovine serum (Gibco), 1% penicillin/streptomycin (Euroclone), 1% L-glutamine (Gibco). Cultures were maintained at 37 °C in a 5% CO₂-humidified atmosphere. IMR90 cells reached replicative senescence in culture after 60 PDL and for this purpose, cells were continually cultured for about 3 months. BJ cells reached replicative senescence in culture at 66 PDL after 4 months of serial passages. Growths were monitored through regular counts of the cell number. The PDLs of cells were calculated by using the following equation: $\log_2(NH/NI)$, where NI is the initial number of cells and NH is the final number of cells at each passage. Cells were plated constantly at a density of 5×10^5 in 10 mm plates and splitted when the plate reaches 90% confluence. Senescence was monitored performing the senescence-associated β -galactosidase (SA- β -Galactosidase) assay and quantifying p21^{WAF1} mRNA levels.

2.2 Induction of premature senescence in IMR90 cells by treatment with Diethylmaleate (DEM) and etoposide.

To induce senescence with DEM (Sigma), young IMR90 cells were plated in complete medium at density of 7×10^5 in 10 mm plates. After 24 h, DEM 100 μ M was added in the medium and cells were grown for 2 days. After this time, the cells were trypsinized, counted, plated at the same densities and treated with the same dose of DEM. Fresh medium plus DEM were replaced at days 4, 6 and 8.

To induce senescence with etoposide, young IMR90 cells were plated in complete medium at density of 1×10^6 in 10 mm plates. The next day was added etoposide (Sigma) directly to the culture medium at a final concentration of 20 μ M, and cells were incubated for another 24 h. Cells were then splitted 1:2 and cultured for 10 days. Fresh medium was replaced every 2 days.

2.3 RNA extraction and Real Time PCR for mRNA

Total RNA was extracted from young/old IMR90 cells, IMR90 cells treated with DEM 100 μ M or with etoposide 20 μ M and BJ young/old cells. In brief, the cell pellet was resuspended and lysed by using Trizol reagent (Invitrogen). Subsequently, the lysate was mixed with an equal volume of chloroform and centrifuged for 5 min at 4°C at 3500 rpm. The supernatant was recovered, added an equal volume of isopropanol, and samples were centrifuged at 3500 rpm for 30 min at 4°C. The pellet containing the total RNA was washed repeatedly with 70% EtOH, centrifuged and resuspended in H₂O. An aliquot of RNA was used to perform qualitative analysis on a denaturing polyacrylamide gel containing urea at a final concentration of 6M and quantitative analysis by spectrophotometry.

The reverse transcriptase reaction (RT) was performed into Gene AMP PCR System 9700. 1 μ g of total RNA was denaturated at 70 °C for 10 min and then incubated at 25 °C for 10 min with mix containing 1X RT buffer with 5 mM MgCl₂, 5 μ M pdN6, 10 mM DTT, 1 mM dNTP, RNase inhibitor 1 U/ μ l and Reverse Transcriptase 10 U/ μ l (M-MLV Reverse Transcriptase, Invitrogen) in a final volume of 20 μ l. These passages are followed by 42°C for 45 min and 99°C for 3 min to degrade RNA and to inactivate the enzyme. The quantitative Real Time PCR was carried out in triplicate with an aliquot of the cDNA (1/10 of RT reactions) in the SYSTEM iCycler supplied of Optical System (Biorad) using iQTM Sybr Green Supermix in triplicate in 25 μ l reaction volumes. The reaction conditions involved a cycle at 95°C for 5 min and 40 cycles with 15 seconds at 95°C and 1 min at 60°C (annealing and amplification). To quantify PCR products, Sybr Green, a dye that binds specifically double-stranded DNA and emits fluorescence, was used. This fluorescence is proportional to the amount of target DNA amplified and it is revealed from the machine during each cycle of amplification. The fluorescence signal, accumulated during the PCR cycles in proportion to the concentration of amplified products, defines for each gene the 'cycle threshold' or Ct, the number of cycles at which the fluorescence reaches a higher value respect to the basic signal. For the quantization was used the comparative $\Delta\Delta$ Ct method by using as a reference gene c-ABL, whose transcript does not vary in our experimental conditions. The PCR reaction was conducted in 25 μ l of which: 12.5 μ l 2X Sybr Green PCR

Master Mix (Biorad); 0.19 μ s 40 μ M forward primer; 0.19 μ s 40 μ M reverse primer; 7.12 μ l H₂O; cDNA(1/10 of RT reactions).

The choice of the primers to use in quantitative Real-Time PCR reactions was performed using the program Primer Express (Perkin-Elmer). The sequences of the primer pairs used were:

c-Abl forward, 5'-TGGAGATAACACTCTAAGCATAACTAAAGGT-3';

c-Abl reverse, 5'-GATGTAGTTGCTTGGGACCCA-3';

p21^{WAF1} forward, 5'-CTGGAGACTCTCAGGGTCGAA-3';

p21^{WAF1} reverse, 5'-CGGCGTTTGGAGTGGTAGAA-3';

Cyclin A forward, 5'-TGGGCACTGCTGCTATGCT-3'; Cyclin A reverse, 5'-TTTCTTGGTGTAGGTATCATCTGTAATGT-3';

Thymidylate synthase (TS) forward, 5'-GAGGAGTTGCTGTGGTTTATCAAG-3';

Thymidylate synthase (TS) reverse, 5'-CCCAGGCTGTCCAAAAAGTC-3';

Cyclin-selective ubiquitin carrier protein (Ucar) forward, 5'-GGGATTTCTGCCTTCCTGA-3';

Cyclin-selective ubiquitin carrier protein (Ucar) reverse, 5'-GCATTGTAAGGGTAGCCACTGG-3'; Interleukin-6 (IL6) forward, 5'-GTACATCCTCGACGGCATCTC-3';

Interleukin-6 (IL6) reverse, 5'-GGTTCAGGTTGTTTTCTGCCA-3';

Hepatocyte nuclear factor-3 (HFH-11A) forward, 5'-AGCCCTTTGCGAGCAGAA-3';

Hepatocyte nuclear factor-3 (HFH-11A) reverse, 5'-CCACTGGATGTTGGATAGGCTAT-3'.

2.4 RNA extraction and analysis of human microRNAs expression

Total RNAs with enriched fraction of small RNAs (200 nucleotides or smaller) were isolated from cultured cells with mirVana miRNA Isolation Kit (Ambion) following the manufacturer's instructions. TaqMan Low Density Arrays (TLDA)/Human microRNA Panels v1.0 (Applied Biosystems), designed for mature microRNA quantification was utilized in our studies to evaluate the microRNA expression. Each card/panel contains primer-probe for 365 human microRNAs present in the Sanger miRBase and three endogenous small RNA controls (RNU48, RNU44 and RNU6). One hundred nanograms of RNA were reverse transcribed using the microRNA multiplex RT primers and the TaqMan microRNA reverse transcription kit (Applied Biosystems). The reaction was incubated for 30 min at 16°C, 30 min at 42°C, and 5 min at 85°C. Each

RT reaction was diluted to 0.5ng/l in the TaqMan Universal PCR Master Mix (Applied Biosystems) and subsequently distributed into the preloaded micro fluidic cards. The reactions were carried out at 50°C for 2 min, followed by 95°C for 10 min, and then by 40 cycles of 95°C for 15 s and 60°C for 1 min. The TaqMan PCR reactions were performed on an ABI Prism 7900HT qPCR system equipped (Applied Biosystems). Cycle threshold (Ct) values were calculated using the automatic baseline and the automatic threshold in *RQ manager v1.1* analysis software. Data were quantified and analyzed using the Sequence Detection System software (v. 2.3) (Applied Biosystems). The value of fold change of each microRNA in senescent versus young cells was obtained by normalizing relative expression of each microRNA against endogenous control RNU6 using the comparative $\Delta\Delta Ct$ method. Ct values > 35 were considered to be below the detection level of the assay. Therefore, only the microRNAs with a Ct \leq 35 were included in the analyses.

2.5 Quantitative PCR Real-Time for microRNAs

For quantitative analysis of microRNAs, two-step TaqMan Real-Time PCR analysis was performed using primers and probes obtained from Applied Biosystems. The TaqMan microRNA assay kit for specific microRNAs was used according to the supplier's protocol.

The reverse transcriptase reaction was performed with 1 μ g of total RNA into the Gene AMP PCR System 9700, using an Applied Biosystems kit (MicroRNA Reverse Transcription). The reaction was conducted in 15 μ l composed of 7 μ l of RT Master Mix, 5 μ l of RNA and 3 μ l of specific primer. The protocol provides a cycle of reaction at 16 °C for 30 min, a cycle at 42 °C for 30 min and a cycle at 85 °C for 5 min. An aliquot of the product of reverse transcription reaction was used to perform Quantitative Real-Time PCR. The conditions of the reaction involved a cycle of reaction at 95 °C for 10 min (activation of the enzyme Taq polymerase) and 40 cycles of 15 seconds at 95 °C and 60 seconds at 60 °C (annealing and amplification).

The PCR reaction was conducted in 20 μ l final in which there is: 10 μ l TaqMan 2X Universal PCR Master Mix; 7.67 μ l H₂O; 1 μ l 20X TaqMan microRNA assay mix; 1.33 μ l of product of RT. RNU6 was used as an endogenous control for microRNAs quantification. Normalized expression of microRNAs was calculated by using the comparative $\Delta\Delta Ct$ method.

2.6 Transfection of IMR90 cells by electroporation

The cells were washed with 1X PBS, trypsinized, counted and centrifuged at $1000\times g$ for 10 min. Cell pellet was resuspended at a density of 1×10^6 cells/0,1 ml buffer R supplied by electroporation kit (Neon Transfection Kit Invitrogen). Electroporation was performed with a MicroPorator MP 100 (Digital Bio) according to the manufacturer's protocol, with some modifications for IMR90 cells. Preliminary experiments were performed to test different conditions of electroporation on IMR90. The selected protocol allows a transfection efficiency of 70% and low SA- β -galactosidase activity (<5%). This protocol consists of 3 pulse each of 1400 Vs for 10 millisecond. For the transient transfections were used synthetic precursors (Applied biosystems) of microRNAs at a final concentration of 100 nM and a pre-miR microRNA negative control precursor was used as a control to compare the activity of others pre-miRs. After transfections cells were seeded on different plates containing coverslips for immunofluorescence analysis. Immediately after electroporation was performed cell counting to estimate the cell mortality caused by electroporation. Since we observed a relatively modest mortality, cell counting was performed comparing number of cells at 48 h and 96 h versus adherent cells counted at 20 h after transfection.

2.7 Bromodeoxyuridine assay

The 5-Bromo-2' deoxy-uridine (BrdU) assay measures cell proliferation. The incorporation of BrdU into the DNA of cells is monitored using a specific monoclonal antibody for BrdU. After transfection, the cells were plated on glass coverslips and after 48 h incubated in presence of BrdU (Roche Diagnostics, Germany) for 48 h at final concentration 10 μ M. The cells on coverslips were fixed at -20°C for 30 min with the ethanol fixative solution (70% EtOH in glycine, pH 2,0) that also permeabilizes the cells. After washing three times with PBS 1X (Roche Diagnostics, Germany) BrdU was detected by covering the cells with the anti-BrdU solution (Roche Diagnostics) for 30 min at 37°C . After washing, the cells were incubated with Alexa Fluor 488-labeled goat antimouse IgG antibody (Invitrogen, Molecular Probes) for 30 min at 37°C , and then washed three times with PBS 1X. The slides are mounted using 10 μ l of a mounting medium that has a counterstain DAPI (4,5 diamidino-2-phenylindole; blue) (Vectashield) that was used to calculate the total number of cells because DAPI counterstained the nuclei.

2.8 Assay for β -galactosidase activity in situ

In situ SA- β -galactosidase staining with 5-bromo-4-chloro-3-indolyl b-D-galactoside (X-gal) was performed as following: the cells were fixed in PBS 1X containing 2% formaldehyde and 0.2% glutaraldehyde for 5 min at room temperature, washed twice with PBS, and then incubated for 24 h at 37°C with 1 mg/ml X-gal dissolved in 40 mM citric acid/sodium phosphate pH 6.0, 5 mM potassium ferrocyanide, 5 mM potassium ferricyanide, 150 mM NaCl and 2 mM MgCl₂. The positive cells were photographed thereafter and scored by assessing at least 300 cells in many random fields/plates.

2.9 Comet assay

DNA damage was evaluated with the Comet assay that was performed according to the manufacturer's protocol. Briefly, transfected cells were washed with PBS 1X, trypsinized, harvested and resuspended in cold PBS 1X. The same procedure was performed on IMR90 cells treated with etoposide at 300 μ M for 4 h, that were used as a positive control. 5×10^3 cells were combined with molten Comet LMAgarose (1% low-temperature melting agarose, Trevigen, Gaithersburg, MD, USA) at a ratio 1:10 (v/v). 60 μ l of the mixture was immediately placed on a CometSlide (Trevigen) and allowed to solidify at 4°C for 20 min. Then cells were lysed by immersing the slides in lysis solution provided by the kit at 4°C for 1 h. Slides were then immersed in a freshly prepared alkaline solution (pH >13) for 40 min and run on a horizontal electrophoresis apparatus for 30 min. After washing in 70% ethanol, the slides were air-dried and kept in the dark until analysis. Cells were visualized by adding 40 μ l of diluted SYBR green and observed under fluorescent microscope. Quantitative analyses of the results were done by using the Image software (National Institutes of Health, Bethesda, MD, USA), as suggested by the manufacturer. Tail moment (TM) was used as descriptor of DNA damage. The tail moment is defined as the product of the tail length and the fraction of total DNA in the tail (TM = tail length x % of DNA in the tail). The comet assay analysis allowed the separation of cells with different categories of DNA damage depending on TM value damage. For these experimental conditions, cells with TM \leq 20 (99% in the negative control of transfected miRs) were regarded as

undamaged (comet classe 0); cells with TM > 20 were considered damaged (comet classes I-V).

2.10 Western blot analysis

Harvested cells were washed twice with ice-cold PBS and centrifuged at 1000×g for 10 min at 4 C. The cell pellet was resuspended in 100µl of ice-cold lysis buffer (0.02 M HEPES pH 7.9, 0.4 M NaCl, 0.1% NP-40, 10% glycerol, 1 mM NaF, 1 mM sodium orthovanadate and a protease inhibitor cocktail). To detect the presence of phosphorylated protein, the buffer for cellular lysis was different: 50 mmol/L HEPES (pH 7.5), 150 mmol/L NaCl, 10% glycerol, 1% Triton X-100, 1 mmol/L EGTA, 1,5 mmol/L MgCl₂, 10 mmol/L NaF, 10 mmol/L sodium PPI, 1 mmol/L Na₃VO₄, 10 µg/ml aprotinin and 10 µg /ml leupeptin. After resuspension, the mixture was clarified by centrifugation at 10000 x g and the supernatant was then used for western blot. Protein concentrations were determined by a Bio-Rad (Italy) protein assay kit. Extracts were subjected to sodium dodecyl sulfate (SDS)-polyacrylamide gel electrophoresis, followed by blotting to nitrocellulose. The blots were probed with antibodies against p21^{WAF1} (Santa Cruz Biotechnology), p16^{INK4a} (Santa Cruz Biotechnology), GAPDH (Santa Cruz Biotechnology), tubulin (Santa Cruz Biotechnology) and phosphorylated CHK1 and CHK2 (Cell signalling) and the signals were detected by using the ECL kit (Amersham Biosciences).

3. RESULTS

3.1 Characterization of replicative senescence in IMR90

IMR90 is a primary cell line of fibroblast derived from human fetal lung that reaches cellular senescence after approximately 60 duplications in vitro. We generated IMR90 senescent cells by serial passages in vitro until the cells exited cycling and acquired a clear senescent phenotype. Figure 5, panel A shows a representative growth curve of IMR90. The cell growth rate was evaluated by calculating PDL (population doubling level) as described in Materials and Methods. Growth curves display a period of exponential trend: in fact up to 45 PDL these cells grow quickly and then begin to slow down and finally after 80 days of culture cells reach a plateau, during which they do not divide but remain metabolically active.

To test the senescent phenotype, we evaluated several markers of the senescence such as the appearance of β -galactosidase activity and the expression levels of some genes related to cell cycle and senescence (6). β -galactosidase is a lysosomal enzyme that in senescent cells accumulates in the cytoplasm and in certain conditions of acid pH (pH 6) its activity can be observed using a chromogenic substrate, 5-bromo-4-chloro-3-indolyl b-D-galactoside (X-gal), that triggers the formation of blue detectable precipitates. The image in the panel B of figure 5 shows that the accumulation of intracellular β -galactosidase activity is proportional to the cumulative PDLs. Furthermore, senescent cells appear morphologically different compared to young cells with an enlarged and flattened morphology.

To further confirm the induction of replicative senescence in IMR90 cells, we evaluated the expression profiles of some genes involved in cell cycle regulation, such as cyclin A, thymidylate synthase (TS), p21^{WAF1} and hepatocyte nuclear factor-3 (HFH-11A), or in pro-inflammatory network (interleukin 6, IL6) as well as in proteasome activity (cyclin-sensitive ubiquitin carrier protein, Ucar). The results were obtained through a quantitative Real Time PCR on total RNA extracted from IMR90 cells at PDL 35 (young control) and IMR90 cells at PDL 60 (senescent cells).

The Figure 5, panel C shows that the mRNAs encoding for cyclin A, thymidylate synthase, Ucar and HFH-11A are many fold decreased in senescent cells compared to young cells, on the contrary p21^{WAF1} and IL6 mRNA levels significantly increased. The results are in agreement with their role in the proliferative exhaustion of senescence.

Finally, the levels of p16^{INK4a} and p21^{WAF1} proteins were assessed by western blot analysis. The panel D in the Figure 5 shows up-regulation of these proteins in IMR90 at PDL 60 indicating a persistent state of cell cycle block.

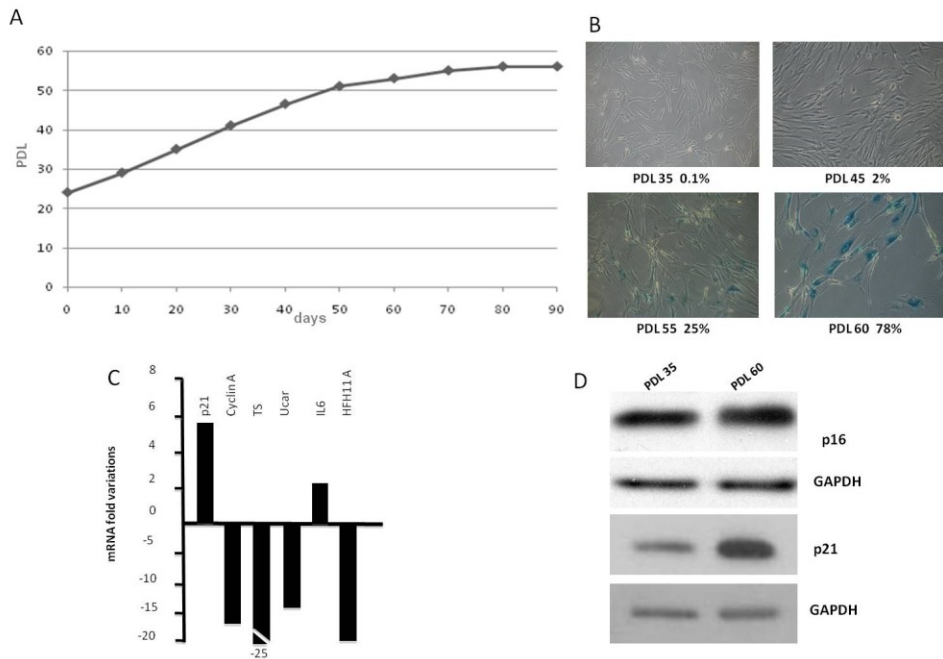


Figure 5: Characterization of replicative senescence in IMR90.

- Representative growth curve of primary human IMR90 fibroblasts. Cells at low passages (PDL 24- *Population Doubling Level*-) obtained from ATCC were continually cultivated until the culture acquired senescence (PDL 60). Cells were plated constantly at a density of 5×10^5 in 10 mm plates and splitted when the plate reached 90% of confluence. The total cell number at each subcultivation was counted and PDL calculated using the equation $X = \log_2 NH/Ni$; NH = final cell number, Ni = starting cell number.
- SA-β-galactosidase staining at different PDLs and relative percentage of coloration. SA-β-galactosidase activity is highlighted by the blue color present in the cytoplasm of cells. The percentages values are obtained by scoring at least 300 cells on the plates. The images also show the different morphology of senescent cells, that appear more flattened, enlarged and granular compared to young cells.
- Changes in mRNA levels of some genes related to cell cycle and senescence. The values in the histogram were obtained by quantitative Real Time PCR comparing the relative mRNA levels of each gene of senescent cells (PDL 60) with those of young cells (PDL 35). For the quantization was used the comparative $\Delta\Delta CT$ method, using as a reference gene c-ABL whose transcript does not vary in our experimental conditions. p21^{WAF1}(p21), cyclin A, thymidylate synthase (TS), cyclin-sensitive ubiquitin carrier protein (Ucar), interleukin-6 (IL6) and hepatocyte nuclear factor-3 (HFH-11A)
- Western Blot analysis of p21^{WAF1} and p16^{INK4a}, two CDK inhibitors, in total protein extracts prepared from young and senescent IMR90 cells. An antibody against GAPDH was used for normalization.

3.2 *microRNA expression profiles in senescent IMR90 fibroblasts*

To assess the expression profile of microRNAs (miRNAs, miRs) in senescent cells we have analyzed a microRNA microarray that probes the expression of 365 known human microRNAs by using RNA extracted from IMR90 senescent cells at PDL 60 and young cells at PDL 35. Experiments were carried out in collaboration with the laboratory of prof. M. Santoro of the Department of Cellular and Molecular Pathology. We used the Taqman Low Density Array (TLDA) that enables the quantitative Real-Time PCR precision in a low-density array format. In each card there are 365 human microRNAs primers spotted and three small RNA controls (RNU48, RNU44 and RNU6). In our microarray study we considered expressed those microRNAs that showed the threshold-cycle (Ct) values below 35 ($Ct < 35$). Applying these criteria 179 microRNAs out of the 284 analyzed were found to be expressed in IMR90 cells. Relative microRNA expression was normalized against the endogenous control RNU6. When compared to young IMR90 cells, senescent IMR90 cells revealed that 47% of microRNA were down-regulated (at least 2 fold) and 19% were up-regulated. It is clear that most of the microRNAs present in the cards do not show changes in their expression levels in senescent cells. The complete set of expression data is reported in Table I.

Among them, we chose to perform further investigations on microRNAs showing higher modifications and with high/medium abundances (below the threshold-cycle value $Ct < 35$), more suitable for accurate microarray data analysis.

miRNA	Fold Change	Induced			
		miRNA	Fold Change	miRNA	Fold Change
hsa-miR-133a-4373142	945	hsa-miR-126-4373269	3,07	hsa-miR-22-4373079	1,5
hsa-miR-200c-4373096	50	hsa-miR-210-4373089	2,93	hsa-miR-152-4373126	1,43
hsa-miR-376b-4373196	44,94	hsa-miR-485-5p-4373212	2,87	hsa-miR-143-4373134	1,43
hsa-miR-9-4373285	26,9	hsa-miR-134-4373141	2,70	hsa-miR-193b-4373185	1,42
hsa-miR-489-4373214	16,54	hsa-miR-449-4373207	2,32	hsa-miR-572-4381107	1,36
hsa-miR-453-4373210	13,31	hsa-miR-656-4380920	2,3	hsa-miR-29c-4373289	1,35
hsa-miR-642-4380995	13,18	hsa-miR-379-4373023	2,21	hsa-let-7f-4373164	1,33
hsa-miR-542-5p-4378105	11,16	hsa-miR-23b-4373073	2,06	hsa-miR-369-5p-4373195	1,3
hsa-miR-184-4373113	6,79	hsa-miR-432-4373280	2,04	hsa-miR-432-4378076	1,27
hsa-miR-486-4378096	6,75	hsa-miR-449b-4381011	1,98	hsa-miR-30c-4373060	1,25
hsa-miR-302d-4373063	6,73	hsa-miR-383-4373018	1,97	hsa-miR-194-4373106	1,24
hsa-miR-189-4378067	6,73	hsa-miR-410-4378093	1,95	hsa-miR-452-4373281	1,22
hsa-miR-337-4373044	6,71	hsa-miR-411-4381013	1,9	hsa-miR-433-4373205	1,22
hsa-miR-182-4373271	6,71	hsa-miR-382-4373019	1,82	hsa-miR-26a-4373070	1,22
hsa-miR-9-4378074	6,67	hsa-miR-30a-5p-4373061	1,82	hsa-miR-452-4378077	1,21
hsa-miR-429-4373203	6,66	hsa-miR-493-4373218	1,78	hsa-miR-503-4373228	1,18
hsa-miR-654-4381014	5,92	hsa-miR-335-4373045	1,71	hsa-miR-629-4380969	1,16
hsa-miR-369-3p-4373032	4,57	hsa-miR-107-4373154	1,65	hsa-miR-323-4373054	1,16
hsa-miR-376a-4378104	4,24	hsa-miR-30a-3p-4373062	1,64	hsa-miR-30d-4373059	1,14
hsa-miR-30e-5p-4373058	3,77	hsa-miR-496-4373221	1,62	hsa-miR-125b-4373148	1,09
hsa-miR-624-4380964	3,38	hsa-miR-491-4373216	1,62	hsa-miR-181c-4373115	1,07
hsa-miR-579-4381023	3,34	hsa-miR-101-4373159	1,60	hsa-miR-485-3p-4378095	1,05
hsa-miR-494-4373219	3,34	hsa-miR-328-4373049	1,6	hsa-miR-137-4373174	1,04
hsa-miR-601-4380965	3,25	hsa-miR-30e-3p-4373057	1,56	hsa-let-7e-4373165	1,04
hsa-miR-139-4373176	3,08	hsa-miR-650-4381006	1,5	hsa-miR-376a-4373026	1,03

miRNA	Fold Change	Repressed			
		miRNA	Fold Change	miRNA	Fold Change
hsa-miR-135b-4373139	0,01	hsa-miR-423-4373015	0,21	hsa-miR-551b-4380945	0,4
hsa-miR-378-4373024	0,01	hsa-miR-340-4373041	0,21	hsa-miR-339-4373042	0,41
hsa-miR-148a-4373130	0,01	hsa-miR-15a-4373123	0,21	hsa-miR-511-4373236	0,43
hsa-miR-616-4380992	0,02	hsa-miR-7-4373014	0,22	hsa-miR-125a-4373149	0,43
hsa-miR-580-4381024	0,02	hsa-miR-28-4373067	0,26	hsa-miR-330-4373047	0,44
hsa-miR-368-4373033	0,02	hsa-let-7b-4373168	0,27	hsa-miR-103-4373158	0,44
hsa-miR-196b-4373103	0,02	hsa-miR-34a-4373278	0,28	hsa-miR-301-4373064	0,46
hsa-miR-142-3p-4373136	0,02	hsa-miR-27a-4373287	0,28	hsa-miR-98-4373009	0,47
hsa-miR-600-4380963	0,05	hsa-miR-213-4373086	0,28	hsa-miR-331-4373046	0,47
hsa-miR-20a-4373286	0,05	hsa-miR-181d-4373180	0,28	hsa-miR-29a-4373065	0,48
hsa-miR-92-4373013	0,07	hsa-miR-130b-4373144	0,28	hsa-miR-374-4373028	0,49
hsa-miR-19b-4373098	0,07	hsa-let-7d-4373166	0,28	hsa-miR-221-4373077	0,49
hsa-miR-200c-4373096	0,08	hsa-miR-34b-4373037	0,29	hsa-miR-186-4373112	0,49
hsa-miR-17-5p-4373119	0,08	hsa-miR-199a-4373272	0,3	hsa-miR-151-4373179	0,49
hsa-miR-15b-4373122	0,09	hsa-miR-342-4373040	0,31	hsa-miR-24-4373074	0,51
hsa-miR-155-4373124	0,09	hsa-miR-222-4373076	0,31	hsa-miR-545-4380918	0,52
hsa-miR-93-4373012	0,1	hsa-miR-565-4380942	0,32	hsa-miR-146a-4373132	0,53
hsa-miR-296-4373066	0,101	hsa-miR-490-4373215	0,32	hsa-let-7a-4373169	0,53
hsa-miR-325-4373051	0,12	hsa-miR-320-4373055	0,32	hsa-miR-361-4373035	0,54
hsa-miR-199b-4373100	0,12	hsa-miR-145-4373133	0,32	hsa-miR-148b-4373129	0,54
hsa-miR-106b-4373155	0,13	hsa-miR-501-4373226	0,33	hsa-miR-21-4373090	0,55
hsa-miR-596-4380959	0,14	hsa-miR-199a-4378068	0,33	hsa-miR-197-4373102	0,55
hsa-miR-502-4373227	0,14	hsa-miR-181b-4373116	0,33	hsa-miR-24-4373072	0,56
hsa-miR-34c-4373036	0,14	hsa-miR-146b-4373178	0,33	hsa-miR-380-5p-4373021	0,57
hsa-miR-16-4373121	0,14	hsa-miR-500-4373225	0,34	hsa-miR-365-4373194	0,57
hsa-miR-192-4373108	0,15	hsa-miR-345-4373039	0,34	hsa-miR-26b-4373069	0,58
hsa-miR-615-4380991	0,17	hsa-miR-299-3p-4373189	0,34	hsa-miR-191-4373109	0,59
hsa-miR-597-4380960	0,17	hsa-miR-20b-4373263	0,34	hsa-miR-140-4373138	0,60
hsa-miR-214-4373085	0,17	hsa-miR-594-4380958	0,35	hsa-miR-425-5p-4380926	0,63
hsa-miR-190-4373110	0,19	hsa-miR-550-4380954	0,36	RNU44-4373384	0,64
hsa-miR-362-4378092	0,2	hsa-miR-425-4373202	0,36	hsa-miR-32-4373056	0,64
hsa-miR-329-4373191	0,2	hsa-miR-324-5p-4373052	0,36	hsa-miR-130a-4373145	0,64
hsa-miR-31-4373190	0,2	hsa-miR-324-3p-4373053	0,37	hsa-miR-409-5p-4373197	0,66
hsa-miR-126-4378064	0,2	hsa-miR-193a-4373107	0,37	hsa-miR-27b-4373068	0,67
hsa-let-7c-4373167	0,200	hsa-miR-532-4380928	0,38	hsa-miR-149-4373128	0,68

Table I: microRNA expression profiles in senescent IMR90 fibroblasts

To assess the expression levels of microRNAs in human senescent IMR90 cells compared to young IMR90 cells was used TaqMan Low Density Arrays TLDA (v 1.0). This method enables the quantitative Real-Time PCR precision in a low-density array format. In each card there are 365 human microRNAs spotted and three small RNA controls (RNU48, RNU44 and RNU6). The results reported in the table I are for the 179 expressed microRNA identified in the cards. For the quantization the comparative $\Delta\Delta CT$ method was performed using as reference the endogenous control RNU6 by using the SDS RQ manager v1.2 software (Applied Biosystems). Effective analysis of these 179 microRNAs shows that 34 microRNAs are up-regulated in senescent cells versus young IMR90 cells and 84 microRNA downregulated (at least 2 fold).

3.3 Validation of microRNA profile in senescent IMR90 fibroblasts

Validation was performed on a selection of the microRNAs identified as differentially expressed by TLDA microarray analysis. We focused on microRNAs showing robust expression (Ct value < 35), which were at least twofold up- or down-regulated. This group included 22 microRNAs derived from the screening that increased in senescent IMR90 cells, 14 microRNAs that decreased during senescence and 2 microRNAs that resulted unchanged (endogenous controls). Selected microRNAs were examined individually by performing quantitative real-time PCR (qRT-PCR) with sequence-specific primers in three different populations of RNAs from young and senescent IMR90 cells. Overall over 80 percent of the microRNAs tested were validated, thus confirming the results generated by the microarray analysis. As shown in Table II, we found that expression of several upregulated microRNAs selected for validation (miR-23b, miR-30e-5p, miR-126*, miR-134, miR-200c, miR-210, miR-369-3p, miR-376a*, miR-379, miR-410, miR-432, miR-485-5p, miR-486, miR-494, miR-542-5p, miR-654 and miR-656), were markedly more abundant in senescent cells as well as selected downregulated microRNAs (miR-7, miR-15b, miR-17-5p, miR-19b, miR-20a, miR-92, miR-93, miR-155, miR-199b, miR-296) were expressed at lower levels in senescent cells. In many cases we observed that related microRNAs, for example microRNAs expressed in polycistronic clusters, showed similar expression profiles. In fact, a common downregulation of members of the 17-92 cluster as well as of the paralogous miR-106 family was found. Interestingly, these clusters very recently were reported to be involved in aging process (114). Similarly, miR-134 (also known as miR-127), miR-369-3p, miR-376a*, miR-379, miR-410, miR-432, miR-485-5p, miR-494, and miR-654, that are overexpressed in senescent IMR90, reside on an imprinted region of human chr. 14q32, that contains more than 50 members and has been found as the largest microRNA cluster to date.

<i>Chr</i>	Induced	Fold change	SD
8	hsa-miR-486-4378096	8,90	0,01
11	hsa-miR-210-4373089	7,90	0,90
1	hsa-miR-30e-5p-4373058	6,50	0,90
14	hsa-miR-376a*-4378104	5,90	0,70
9	hsa-miR-126*-4373269	5,42	1,40
14	hsa-miR-494-4373219	4,50	1,60
14	hsa-miR-379-4373023	4,40	1,60
14	hsa-miR-654-4381014	4,36	1,40
X	hsa-miR-542-5p-4378105	3,70	0,60
14	hsa-miR-432-4373280	3,70	0,60
14	hsa-miR-369-3p-4373032	3,30	0,40
9	hsa-miR-23b-4373073	3,30	1,00
14	hsa-miR-134-4373141	3,20	1,00
14	hsa-miR-410-4378093	3,10	0,40
14	hsa-miR-485-5p-4373212	2,70	0,50
14	hsa-miR-656-4380920	2,59	0,60
12	hsa-miR-200c-4373096	1,70	0,50
<i>Chr</i>	Repressed	Fold change	SD
13	hsa-miR-20a-4373286	0,13	0,01
21	hsa-miR-155-4373124	0,14	0,04
13	hsa-miR-17-5p-4373119	0,15	0,02
13	hsa-miR-92-4373013	0,20	0,04
13	hsa-miR-19b-4373098	0,20	0,10
3	hsa-miR-15b-4373122	0,20	0,16
20	hsa-miR-296-4373066	0,20	0,20
9	hsa-miR-199b-4373100	0,20	0,09
9	hsa-miR-7-4373014	0,28	0,13
7	hsa-miR-93-4373012	0,35	0,04

Table II: Validation of senescence-associated microRNA profiles in IMR90 cells.

TaqMan microRNA assays (Applied Biosystems) were performed on selected microRNAs to validate the microarray results. For the analysis, microRNAs that were significantly upregulated or downregulated (at least 2 fold) in IMR90 PDL60 versus PDL 35 and expressed at Ct < 35 were chosen. The reported fold changes were normalized to RNU6. The data shown are the mean \pm standard deviation of three independent experiments carried out on three different populations of IMR90 derived from three different original cultures. The microRNAs in the table are listed according to their descending fold change values. The chromosomal localization of the microRNA is also indicated.

3.4 Senescence-associated microRNA profiles in BJ cells and in premature senescent IMR90 cells

To assess whether these microRNAs alterations are more closely related to replicative senescence of IMR90 or may be considered as a common phenomenon in other types of replicative or premature senescence, we used another example of replicative senescence obtained in BJ cells, a human cell line from foreskin fibroblasts that reach a state of senescence after a greater number of cell duplication (PDL 66). As shown by Figure 6 both the phenotype and the evolution of senescence markers are very similar to IMR90. Indeed, in the panel A it is showed that the accumulation of intracellular β -galactosidase activity is comparable to β -galactosidase activity in IMR90 cells. Also the expression profiles of genes involved in cell cycle regulation, such as cyclin A, thymidylate synthase (TS), p21^{WAF1} and HFH-11A, or in pro-inflammatory network (interleukin 6, IL6) as well as proteasome activity (cycline-sensitive ubiquitin carrier protein) and the protein levels of p21^{WAF1} and p16^{INK4a} are similar to those observed in senescent IMR90 cells (Figure 6, panels B and C).

We quantified the levels of those microRNAs that showed significant expression differences based on the microarray results and that were validated in senescent IMR90 cells. qRT-PCR for single mature microRNAs was employed to compare microRNA expression patterns of senescent (PDL 66) BJ cells versus young proliferating cells (PDL 30). As shown by Figure 6, Table III, in BJ cells, with the exception of miR-410 and miR-654 (up-regulated), miR-199b and miR-296 (down-regulated), that showed a less pronounced change in senescent BJ cells, all other microRNAs showed a general trend of variations that overlapped with IMR90 cells. These results indicate that these selected up- or down-regulated microRNAs exert a biological action in the senescence program.

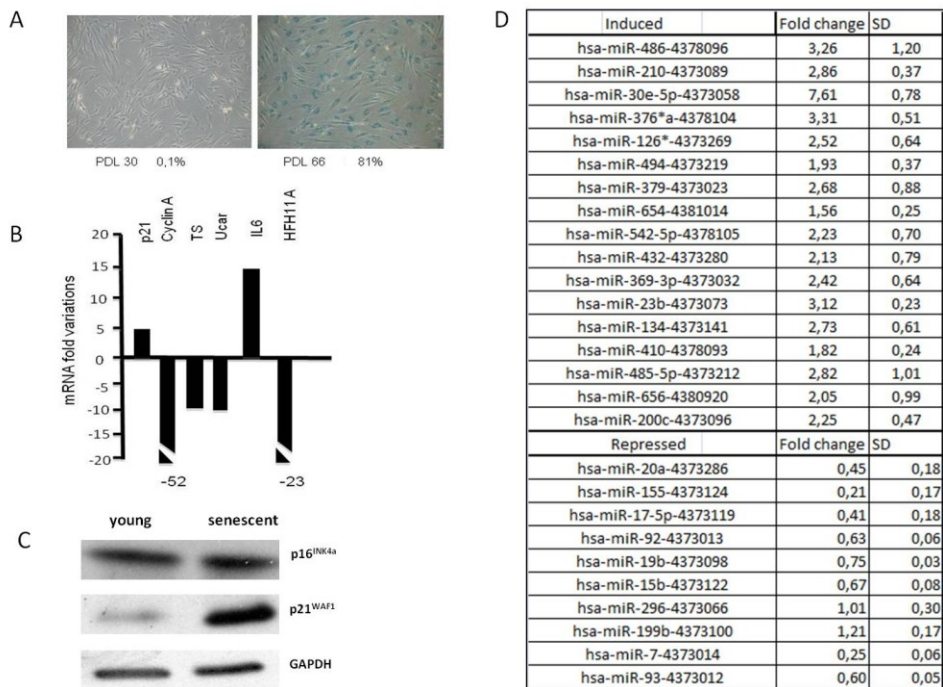


Figure 6: Senescence-associated microRNA profiles in BJ cells.

A) Representative images of SA- β -galactosidase staining in primary human BJ cells at PDL 30 and PDL 66 and relative percentage of coloration. SA- β -galactosidase activity is highlighted by the blue color present in the cytoplasm of cells. The values of the percentages are obtained by scoring at least 300 cells on the plates.

B) Changes in mRNA levels of some genes related to cell cycle and senescence. The values in the histogram were obtained by quantitative Real Time PCR comparing the relative mRNA levels of each gene of senescent cells (PDL 66) with those of young cells (PDL 30). For the quantization was used the comparative $\Delta\Delta$ CT method, using as a reference gene c-ABL whose transcript does not vary in our experimental conditions. p21^{WAF1}, cyclin A, thymidylate synthase (TS), cyclin-sensitive ubiquitin carrier protein (Ucar), interleukin-6 (IL6) and hepatocyte nuclear factor-3 (HFH-11A).

C) Western Blot analysis of p21^{WAF1} and p16^{INK4a}, two CDK inhibitors, in total protein extracts prepared from young and senescent BJ cells. An antibody against GAPDH was used for normalization.

Table III: TaqMan microRNA assays (Applied Biosystems) were performed on selected microRNAs to assay their expression levels in replicative senescent BJ cells (PDL66 versus PDL30). The reported fold changes were normalized to RNU6. The data shown are the mean \pm standard deviation of three independent experiments.

Because senescence in human cells can be triggered by both intrinsic factors such as telomere regression and extrinsic factors such as oncogenic stress, DNA damage, and oxidative stress, we determined microRNA expression signatures in IMR90 premature senescence induced by chronic oxidative stress (SIPS) or by DNA damaging agent (DDPS). To find common participants involved in senescence, young IMR90 fibroblasts (PDL35) were chronically exposed for 10 days to low doses of the GSH-depleting agent DEM (100 μ M) (115) or treated for 24 h with etoposide (20 μ M) and then maintained in culture for 10 days (see Materials and Methods). Under these conditions, IMR90 cells acquired a senescent phenotype resembling that observed after serial *in vitro* passages, as confirmed by the analysis of the expression profiles of genes involved in cell cycle regulation or in pro-inflammatory network as well as proteasome activity that are similar to those observed in replicative senescent IMR90 cells (Figure 7 panels A, B). Also, the levels of p21^{WAF1} proteins were assessed by western blot analysis and these levels are increased after treatments (Figure 7 panels C). The microRNA expression signatures in DEM-senescent and in etoposide-senescent IMR90 compared to untreated cells, carried out by qRT-PCR method, is summarized in Figure 7, Table IV. In IMR90 cells treated with DEM 100 μ M or etoposide 20 μ M, with the exception of miR-200c, miR-542-5p and miR-656 that were unchanged in both conditions (cut off 1,5 fold), most of the microRNAs analyzed in SIPS and DDPS showed similar expression modifications relative to *in vitro* exhaustion of replicative capacity.

In this part of the study we were able to identify a large set of microRNAs, the expression of which constitutes a recurring signature of senescence, independently from cellular context and stimuli. These results indicate that senescence follows a common molecular program in microRNA expression.

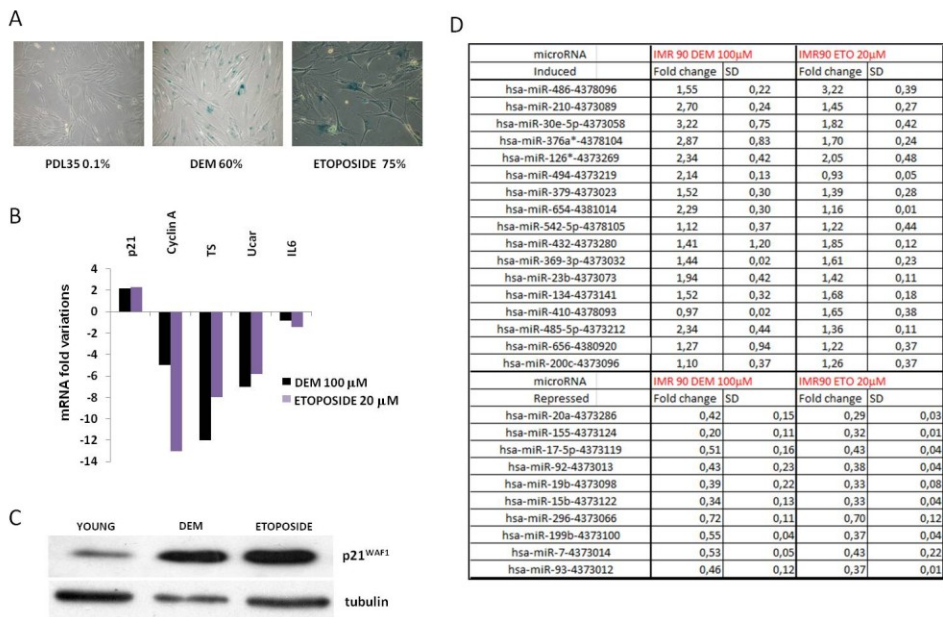


Figure 7: Senescence-associated microRNA profiles in premature senescent IMR90 cells

A) Representative images of SA- β -galactosidase staining in IMR90 cells at PDL 35 (control cells), after treatment with 100 μ M DEM for 10 days or 20 μ M etoposide for 24 h, splitted 1:2 and left in culture for 10 days and relative percentage of coloration. SA- β -galactosidase activity is highlighted by the blue color present in the cytoplasm of cells. The values of the percentages are obtained by scoring at least 300 cells on the plates.

B) Changes in mRNA levels of some genes related to cell cycle and senescence after 10 days of treatment with 100 μ M DEM and after treatment with 20 μ M etoposide for 24 h and cultured for 10 days. The values in the histogram were obtained by quantitative Real Time PCR comparing the relative mRNA levels of each gene of treated cells with those control cells. For the quantization was used the comparative $\Delta\Delta$ CT method, using as a reference gene c-ABL whose transcript does not vary in our experimental conditions. p21^{WAF1}, cyclin A, thymidylate synthase (TS), cyclin-sensitive ubiquitin carrier protein (Ucar) and interleukin-6 (IL6).

C) Western Blot analysis of p21^{WAF1}, a CDK inhibitors, in total protein extracts prepared from treated cells and control cells. An antibody against tubulin was used for normalization.

Table IV: TaqMan microRNA assays (Applied Biosystems) were performed on selected microRNAs to assay their expression levels in premature senescent induced in IMR90 with treatment with 100 μ M DEM and 20 μ M etoposide. The reported fold changes were normalized to RNU6. The data shown are the mean \pm standard deviation of three independent experiments.

3.5 Overexpression of some selected up-regulated microRNAs inhibits cell growth in IMR90 cells

To investigate whether the variation of levels of these microRNAs is a causative event of senescence or a consequence of intracellular pathway disturbance after the onset of senescence, we set up functional experiments. Since most of the studies have focused on downregulated microRNAs, we decided to overexpress selected upregulated microRNA in young IMR90 with the rationale that elevated levels of these microRNAs could induce a senescence program.

To this aim we transfected synthetic precursor of microRNAs (pre-miRs, Applied Biosystems) in IMR90 cells at PDL 35. For transfection experiments we selected 12 upregulated microRNAs (miR-30e-5p, miR-126*, miR-200c, miR-210, miR-376a*, miR-369-5p, miR-379, miR-432, miR-486, miR-494, miR-542-5p, miR-654), and an unmodified microRNA (miR-32).

The precursors used are double-stranded RNAs chemically modified, designed to be incorporated into the effector complex RISC and thereby mimic endogenous mature microRNAs. As shown in Figure 8, panel B, a Cy3 dye-labeled negative pre-miR allows the monitoring of transfection efficiency, that was calculated 70% in our experimental conditions.

To obtain a quantization of levels of mature microRNAs and a time-course of its maturation, we performed quantitative Real Time PCR on RNA extracted from transfected cells at 24 h, 48 h and 96 h after transfection, using specific TaqMan probes (Applied Biosystems). As shown in Figure 8, panel C, the intracellular levels of representative mature microRNAs (miR-210) significantly increased in cells transfected with the pre-miRNA (300-500 fold) and peaks at 48 h after transfection.

To analyze the effects of the different pre-miRs in young IMR90 cells (PDL 35), we analyzed various parameters related to the senescent phenotype. First, we evaluated cell proliferation by performing cell counting at 48 h and 96 h after transfection and compared them to the number of adherent cells at 24 h. As shown in Figure 8, panel A, the number of cells transfected with pre-miRs 210, 376a*, 486, 494, 542-5p and 654, at 48 h and 96 h after transfections shows a clear reduction of growth, already at 48 h after transfection, which persist at 96 h. On the contrary, some pre-miR overexpressions (pre-miRs 30e-5p, 32-unchanged control-, 126*, 200c, 369, 379 and 432) have no effect on cell growth of young IMR90 cells.

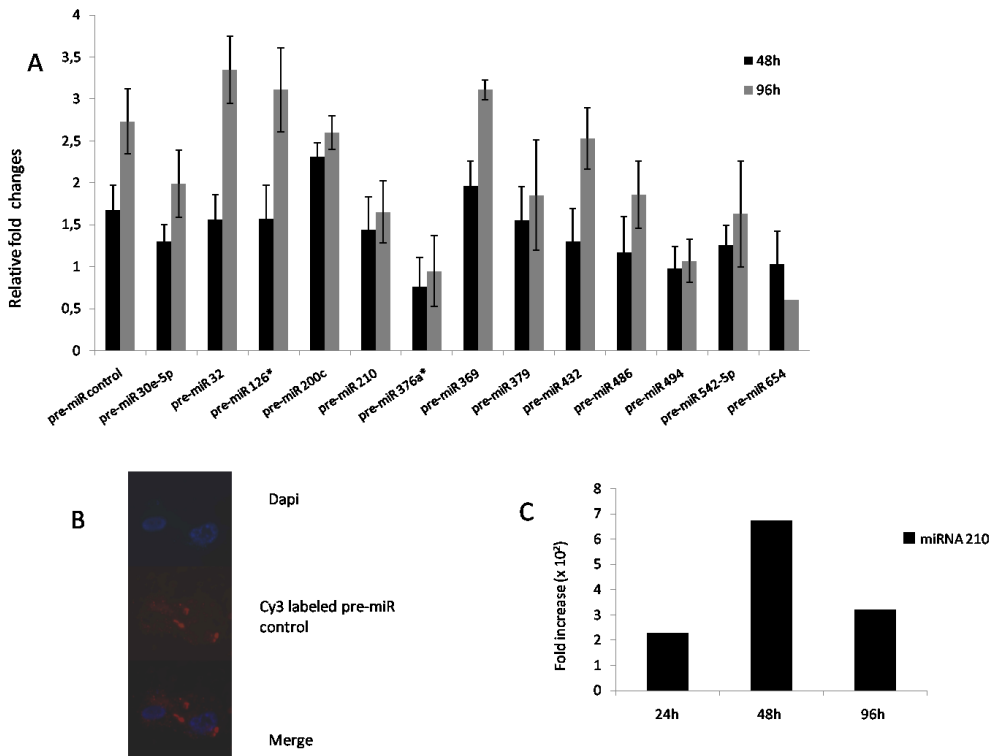


Figure 8: Overexpression of some selected up-regulated microRNAs inhibits cell growth in IMR90 cells

A) Cell counting. Transient transfections with precursor molecules of microRNAs (pre-miRs) that were up-regulated in senescent cells were made in young IMR90 (PDL 35) cells. Pre-miRs were used at a final concentration of 100 nM. A pre-miR miRNA negative control precursor were used as a control to compare the activity of others pre-miRs. Histograms show the fold variations of cell number obtained by comparing the number of adherent cells at 48/96 h with the number of adherent cells at 24 h after transfection. The data obtained are the mean \pm standard deviation of at least three independent experiments.

B) Pre-miRs transfection efficacy. Cy3 dye-labeled pre-miR Negative Controls (Ambion) was viewed with a fluorescent microscope at 24 h after transfection. Nuclei are been displayed with DAPI.

C) Representative Taq-Man assay performed on miR-210 to assay its expression levels and a time course of its maturation in transfected IMR90 young cells at 24 h, 48 h and 96 h after transfections. The reported fold changes were normalized to RNU6.

This demonstrates that it is not the overexpression of microRNA *per se* and consequently the perturbation of the microRNA processing machinery that blocks cell growth.

To assess the amount of cells that are in active proliferation, we analyzed the incorporation of bromodeoxyuridine (BrdU), an analogue of thymine that is incorporated during DNA synthesis after transfection of cells. Because IMR90 young cells have a relatively long doubling time (about 36 hours), we incubated the cells with BrdU for 48 h. Immunofluorescence experiments using an antibody directed against BrdU were performed at 96 h after transfections. Figure 9, panel A indicates that cells transfected with pre-miR 210, 376a*, 486, 494, 542-5p, 654 have a remarkable reduction of DNA synthesis, perhaps associated with a block of cell cycle in G1 phase. On the contrary, cells transfected with pre-miRs 30e-5p, 32, 126*, 200c, 369, 379 and 432 have a rate of incorporation of BrdU similar to that observed in cells transfected with pre-miR negative control. Representative immunofluorescence are presented in Figure 9, panel B.

The data reported indicate that some selected microRNAs found overexpressed in the initial screening inhibit cell growth, probably in G1/S phase. It is important to specify that in one case, miR-654, the amount of alive cells after 96 h from transfection is much lower in comparison to the amount of alive cells at 24 h and in the other samples at the same time, indicating that the most important role of this microRNA could be related to cell death.

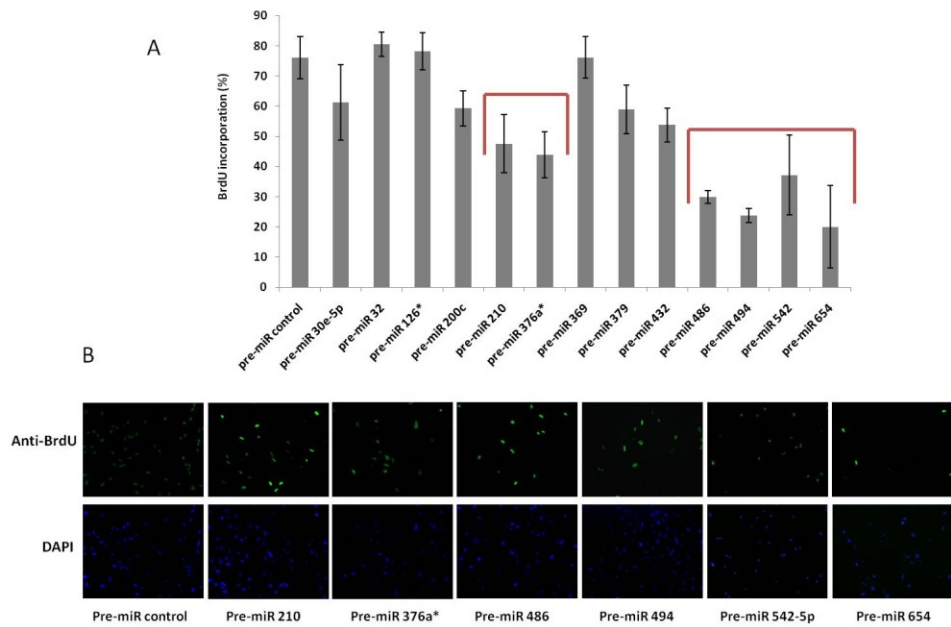


Figure 9: Bromodeoxyuridine (BrdU) labeling in cells over-expressing selected microRNAs
 A) Quantitative analysis of BrdU positive cells. Histograms show the percentage of BrdU-positive IMR90 cells transfected with different pre-miRs evaluated at 96 h after a 48 h of pulse time. The data obtained are the mean \pm standard deviation based of three independent experiments.
 B) Assay of BrdU incorporation in cells transfected with pre-miRs. The images show representative transfected cells immunostained with anti-BrdU antibody and counter stained with DAPI to visualize DNA. Images were collected by fluorescent microscopy.

3.6 Overexpression of some selected microRNAs induces a senescent-like phenotype

From the above experiments resulted that various microRNAs (miR-210, miR-376a*, miR-486, miR-494, miR-542-5p and miR-654) are able to inhibit cell cycle progression with reduced BrdU incorporation. To test the hypothesis that these microRNAs are able to induce the senescence program, we analyzed the β -galactosidase activity, more linked to senescence in cells transfected with these microRNAs. To this aim we performed β -galactosidase staining in cells overexpressing the above mentioned pre-miRs at 7 days after transfection. Quantification of the data showed that the β -galactosidase activity in cells transfected with pre-miRs 210, 376a*, 486, 494, 542-5p significantly increases, with staining values that range from 10 to 25 positiveness percentage compared to 1 percent of the control, as shown in Figure 10, panel A. Representative SA- β -galactosidase staining of cells transfected with these microRNAs are presented in Figure 10, panel B.

Another evidence of the induction of senescence comes from the morphology of the transfected cells, at least in those with more elevated β -galactosidase activity. These cells show enlarged cell size, a loss of filamentous morphology typical of human fibroblasts and an irregular cellular margin. Cells transfected with pre-miR 486 instead show an unusual phenotype with small size and a reduced cytoplasm. Cells transfected with pre-miR 654 are numerically lower compared to other cells and show a pyknotic and very stressed morphology.

Following data were obtained in collaboration with the group of prof. M. Santoro of the department of Biology and Cellular and Molecular Pathology. The data concerned the presence of senescence-associated foci (SAHFs) by immunofluorescence experiments in cells transfected with above mentioned pre-miRs at 7 days after transfection. The presence of SAHFs at 7 days was visualized by using an anti-3meH3K9 antibody. This immunofluorescence analysis shows the presence of SAHFs in 8-21% of IMR90 cells transfected with pre-miRs 210, 376a*, 486, 494, and 654, compared to 4% of negative control and compared to 36% of positive control, such as IMR90 cells at PDL 60 (data not shown).

The results reported above indicate that the overexpression of the pre-miRs 210, 376a*, 486, 494, 376a*, 542-5p and 654 could be correlated with the onset of senescence.

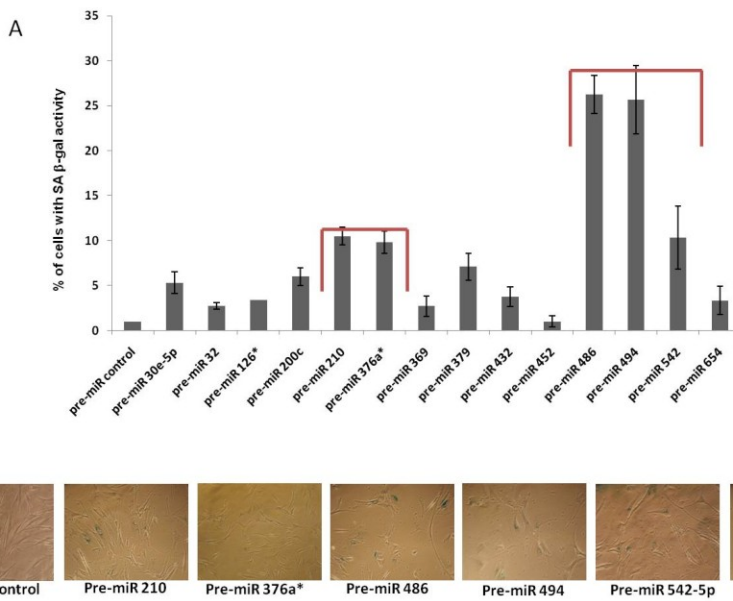


Figure 10: Overexpression of selected microRNAs induces a senescent-like phenotype

A) Quantification of SA-β-galactosidase-positive IMR90 cells transfected with selected pre-miRs analyzed at 7 days after transfection. The data obtained are the mean ± standard deviation of three independent experiments. At least 300 cells were scored for quantification of positive cells.

B) The images show SA-β-galactosidase activity in representative IMR90 cells transfected with the pre-miRNAs, which showed elevated β-galactosidase activity.

3.7 *Senescent-like phenotype is related to a persistent DNA damage*

Given that senescence program encompasses a canonical DNA damage checkpoint, we next investigated whether microRNA-induced senescence in IMR90 cells is correlated with the DNA damage.

To evaluate the extent of DNA damage induced by the microRNAs, we used comet assay in alkaline conditions detecting both single strand breaks (SSB) and double strand breaks (DSB). DNA strand breaks in transfected cells were quantified using imaging software analysis by calculation of tail moment (TM), the product of the percentage of DNA in the tail and tail length (TM = tail length x % of DNA in the tail). Data collected for each population of etoposide-treated cells (positive control) and transfected cells showed different categories of DNA damage depending on TM value damage. Comet images illustrating the visual scoring classification are showed in Figure 11, panel B. The data analysis, reported in Figure 11, panel A, detects damaged DNA (cells with TM > 20) in 8-40% of IMR90 cells transfected with miR-210, miR-376a*, miR-486, miR-494, miR-654, compared to less than 1% of pre-miR negative control (TM < 20) at 96 h after transfection. Remarkably, for some of these microRNAs not only the damage persists at 7 days but it also increased (miR-210, miR-486, miR-494).

Other data obtained in collaboration with the group of prof. M. Santoro have confirmed these results. The data concerned the presence of histone H2AX phosphorylated (γ H2AX) by immunofluorescence experiments in cells transfected with above mentioned pre-miRs at 7 days after transfections. This is the histone H2A-variant that becomes phosphorylated (in serine 139) in chromatin regions flanking double strand breaks (DSB) sites and it is used as a marker of persistent DNA damage. This immunofluorescence analysis shows the presence of γ H2AXs in 28-34% of IMR90 cells transfected with pre-miRs 210, 486, 494 and 654 compared to 12% of negative control (data not shown).

We also investigated if markers of DNA damage such as phosphorylated CHK1 and CHK2 are present in cellular extracts from transfected cells at 96 h after transfections. Very preliminary results obtained by western blot analysis showed the presence of phosphorylated CHK1 and/or CHK2 in cells overexpressing the above mentioned microRNAs (data not shown).

Together, our data indicate that miR-210, miR-376a*, miR-486 and miR-494 induced cellular senescence that may be mediated in part by activation of DNA damage pathway.

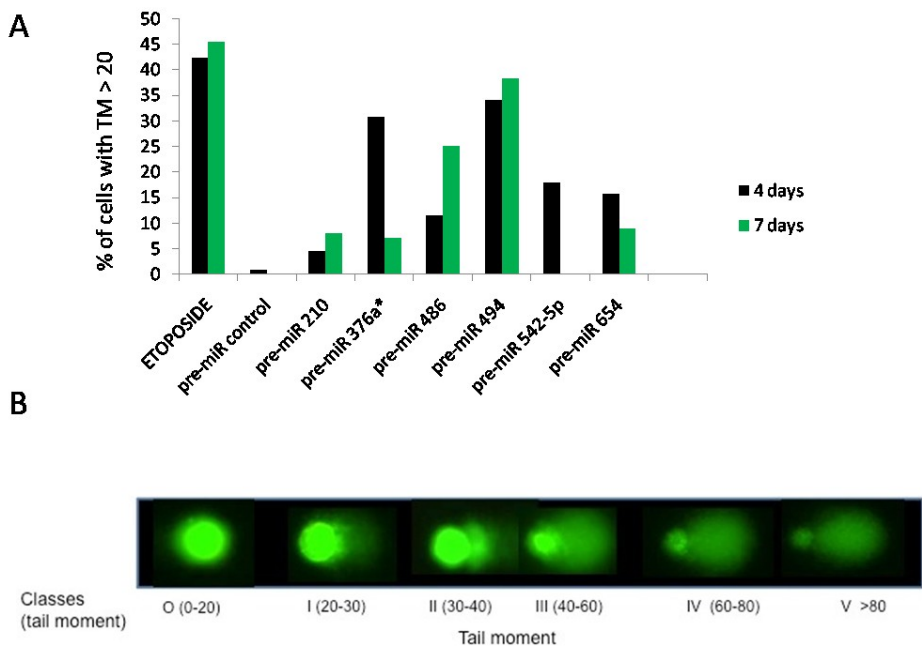


Figure 11: Senescent-like phenotype is related to activation of a persistent DNA damage

A) DNA damage quantification in IMR90 cells transfected with the different pre-miRs. Histograms show the percentage of cells having tail moment (TM) > 20 at 96 hours and 7 days after transfection with the indicated pre-miRs. Cells treated with etoposide 300 μ M for 3 hours were used as a positive control. The tail moment is defined as the product of the tail length and the fraction of total DNA in the tail and it is calculated automatically by the computer software system for each cell analyzed (we scored at least 100 cells). For these experimental conditions, cells with TM \leq 20 were considered as undamaged (comet class 0); cells with TM >20, were considered damaged (comet classes I-V).

B) The images show the visual scoring classification. Classes represent increasing DNA damage reflected by the increasing tail moment.

3.8 Prediction of targets of Senescence-Associated microRNAs (SA-microRNAs) involved in pathway correlated to cellular senescence.

We examined pathways involved with cellular senescence that could be regulated by SA-microRNAs, in particular we analyzed putative targets for four regulatory pathways: regulation of cell cycle/growth arrest, chromatin remodeling, DNA damage/repair and apoptosis.

We have researched predicted targets using the algorithm Targetscan (<http://www.targetscan.org>). From Table V it is obvious that most of the predicted targets are related to cell cycle/growth arrest pathways. Remarkably, some microRNAs (376a*, 494) may also target mRNAs involved in the repair of DNA damage. This evidence is in accord with our results that demonstrate that the induction of like-senescence phenotype after transfection of microRNAs is related to a persistent DNA damage. miR-376a* targets the polymerase mRNA theta that cooperates with polymerase beta in base excision repair of oxidative DNA damage (116). miR-494 targets the Cul4a mRNA. This protein is involved in the repair of DNA damage: in fact Cul4a is associated with other molecules to form the complex cullin-RING ubiquitin E3-ligase (CRL), which is recruited at sites of DNA damage and also is important for subsequent DNA repair.

Furthermore, despite miR-210 does not target known DNA-damage related mRNAs, it was recently reported that ISCU (Iron Sulfur Cluster homolog) proteins, involved in mitochondrial function, are targets of this microRNA (118). This leads to increased ROS, thereby affecting DNA homeostasis. Interestingly, microRNA 654, which induced a decrease in cell number in IMR90 after transfection, targets a mRNA involved in apoptosis, TRAF 4 that acts as anti-apoptotic factor and its reduction correlates with an increase of apoptosis.

microRNA	cell cycle/ growth arrest	DNA damage/repair	chromatin remodeling	apoptosis
microRNA 210		<i>ISCU, NDUFA4</i>		
microRNA 376a*	CHD9, FGF5	POLQ	HDAC9	BCL11A, PRKCI
microRNA 486	MAPK3, IMPDH1, PI4K2A		PHF8, JMJD3	TNFRSF1B, DDX26B
microRNA 494	CDK6, CCNT2, PTEN, ZFH3, SEPT9, PPM1B, SIRT1, PPP2R2B, ACVR1C, CKS1B, NFIB, RPRD1A, CHD1, CCND2, PPP2R5E	CUL4A	ATRX, PHF8, SAP18, SMARCE1, CHD1, H3F3A, H3F3B, PHF15	BBC3, UACA, SIRT1, XIAP
microRNA 654	STK38, ARAF		WDR82, KDM6B	TRAF 4

Table V: Prediction of targets of Senescence-Associated microRNAs (SA-microRNAs). Predicted targets of SA-microRNA involved in 4 pathways related to cellular senescence (growth arrest/cell cycle, DNA damage/DNA repair, chromatin remodeling, apoptosis). For the prediction TargetsCan algorithm (www.targetscan.org) was used. ISCU and NDUFA4 are in italic because they are indirectly related to DNA damage.

4. DISCUSSION/CONCLUSIONS

MicroRNAs (miRNAs or miRs) are small non-coding RNAs that act as post-transcriptional regulators of gene expression, resulting in suppression of translation or degradation of target mRNAs. It is believed that around 60% of human genes coding for proteins are regulated by microRNAs. microRNAs resemble the transcription factors that influence many cellular responses because each microRNA can have up to hundreds of targets. Consistent with this, microRNAs are involved as regulators virtually in many networks, including development, proliferation, apoptosis and cancer. Similarly, emerging evidence indicate a role for microRNAs in regulating senescence.

We explored the involvement of microRNAs in the induction and maintenance of cellular senescence.

The results presented in this thesis show that several microRNAs are differentially expressed during replicative senescence of primary human IMR90 cells. These data were then validated by Real Time PCR experiments in replicative senescent cells derived from fetal lung (IMR90) or neonatal foreskin (BJ) and in premature senescence induced in young IMR90 cells by oxidative stress caused by DEM or DNA damage induced by etoposide.

We have chosen 12 microRNAs up-regulated in senescent cells to study their functional role in the induction of the senescent phenotype. To this purpose we performed overexpression experiments in IMR90 cells at PDL 35 (young fibroblasts) by transfecting synthetic precursors of selected microRNAs (pre-miRs). Thus, we evaluated markers of cellular senescence following the overexpression of these microRNAs. Our results have shown that many selected upregulated microRNAs induce growth arrest and block of DNA synthesis already at 96 hours after transfections, at which time there is greater activity of the transfected microRNAs.

Furthermore we evaluated β -galactosidase activity. Some microRNAs (miR-210, miR-376a*, miR- 486, miR-494, miR-542-5p, miR-654) appear to play a causative role in senescence: cells transfected with these pre-miRs acquire a senescent-like phenotype as demonstrated by the presence of β -galactosidase activity and by presence of several molecular markers, such as SAHFs.

One of the principal causes of senescence is the presence of DNA damage not repairable. Here we investigated whether overexpression of selected microRNAs coincides with the presence of DNA damage that

mainly governs the induction and the establishment of senescence. The extent of DNA damage analyzed by comet assay and immunofluorescent experiments for specific foci of γ H2AX show that in some cases the damage induced by overexpression of microRNAs persists at 7 days after transfection. This could be the critical determinant that leads some microRNAs (miR-210, miR-376a*, miR-486, miR-494 and miR-654) to induce a senescent-like phenotype.

Finally, senescence-inducing molecular pathways in which these microRNAs may be involved were proposed using computational target prediction algorithms. We focused on 4 pathways related to cellular senescence: cell cycle/growth arrest, chromatin remodeling, apoptosis and DNA damage. Many predicted target mRNAs are linked to these different pathways, in particular to cell cycle. It will be of interest to explore if these proteins are downregulated after overexpression of these pre-miRs. Taken together, the functions of senescence-associated microRNAs need to be better investigated. It would be also important to see if a reduced expression of these microRNAs in pre-senescent cells implies a delay in the induction of senescent phenotype.

Another aspect that remains to be investigated is the study of microRNAs resulting downregulated from the screening. For these microRNAs we propose that functional experiments can be performed by using anti-miR in young IMR90 cells to reduce endogenous microRNA levels and to analyze if they or some of them are able to induce a senescence phenotype. Furthermore it could be of interest to explore if overexpression of downregulated pre-miRs in pre-senescent cells can delay the appearance of the senescence.

Finally, related to basic and biomedical aging research, of particular interest it will be to explore the possibility that some of these microRNAs may be used as markers of aging and of the onset of age-related diseases.

5. REFERENCES

1. Smith JR, Pereira-Smith OM. *Replicative senescence: implications for in vivo aging and tumor suppression*. Science 1996; 273:63-7.
2. Hayflick, L. *The limited in vitro lifetime of human diploid cell strains*. Exp. Cell. Res. 1965; 37: 614-636.
3. Cong YS, Wright WE, Shay JW. *Human telomerase and its regulation*. Microbial Mol 2002; 66: 407-425.
4. Krtolica A, Parrinello S, Lockett S, Desprez PY, Campisi J. *Senescent fibroblasts promote epithelial cell growth and tumorigenesis: a link between cancer and aging*. Proc natl acad sci USA 2001; 98:12072-7.
5. Hayflick, L. *How and why we age*. Ballantine Books, New York 1994.
6. Stein GS, Baserga A, Giordano A, Denhardt DT. *The molecular basis of cell cycle and growth control*. Wiley-Liss, New York, 348-373.
7. Bayreuther K, Rodemann HP, Hommel R, Dittmann K, Albiez M, Francz PI. *Human skin fibroblasts in vitro differentiate along a terminal cell lineage*. Proc Natl Acad Sci USA 1988; 85 (14):5112-5116.
8. DJ Kurz, S Decary, Y Hong, JD Erusalimsky. *Senescence-associated β -galactosidase reflects an increase in lysosomal mass during replicative aging of human endothelial cells*. J Cell Sci 2000; 113: 3613–362.
9. Dimri GP, Lee X, Basile G, Acosta M, Scott G, Roskelley C, Medrano EE, Linskens M, Rubelj I, Pereira-Smith O. *A biomarker that identifies senescent human cells in culture and in aging skin in vivo*. Proc Natl Acad Sci USA 1995; 92(20):9363-9367.
10. Narita M, Nunez S, Heard E, Narita M, Lin AW, Hearn SA, Spector DL, Hannon GJ, Lowe SW. *Rb-mediated heterochromatin formation and silencing of E2F target genes during cellular senescence*. Cell 2003; 113, 703-716.
11. Lars Zender, K. Lenhard Rudolph. *Keeping your senescent cells under control*. Aging, May 2009.
- 12 Hampel B, Malisan F, Niederegger H, Testi R, Jansen-Durr P. *Differential regulation of apoptotic cell death in senescent human cells*. Exp. Gerontol. 2004, 39: 1713–1721.
13. Rebbaa A, Zheng X, Chou PM, Mirkin BL. *Caspase inhibition switches doxorubicin-induced apoptosis to senescence*. Oncogene 2003, 22: 2805–2811.

14. Campisi J. *Cellular senescence and apoptosis: how cellular responses might influence aging phenotypes*. Exp. Gerontol. 2003, 38: 5–11.
15. Seluanov A et al. *Change of the death pathway in senescent human fibroblasts in response to DNA damage is caused by an inability to stabilize p53*. Mol. Cell. Biol. 2001, 2: 1552–1564.
16. Jackson JG, Pereira-Smith OM. *p53 is preferentially recruited to the promoters of growth arrest genes p21 and GADD45 during replicative senescence of normal human fibroblasts*. Cancer Res. 2006, 66: 8356–8360.
17. Andrew RJ Young, Masako Narita, Manuela Ferreira. *Autophagy mediates the mitotic senescence transition*. Genes & Dev. 2009; 23: 798-803.
18. Moyzis RK, Buckingham JM, Cram LS, Dani M, Deaven LL, Jones MD, Meyne J, Ratliff RL, Wu JR. *A highly conserved repetitive DNA sequence, (TTAGGG)_n, present at the telomeres of human chromosomes*. Proc Natl Acad Sci USA 1988; 85(18):6622-6626.
19. Lars Zender¹, Lenhard Rudolph. *Keeping your senescent cells under control*. Aging, May 2009, Vol. 1 No. 5.
20. Shay JW, Pereira-Smith OM, Wright WE. *A role for both RB and p53 in the regulation of human cellular senescence*. Exp Cell Res 1991, 196: 33–39.
21. Sharpless NE, DePinho RA. *The INK4A/ARF locus and its two gene products*. Curr Opin Genet Dev 1999, 9: 22–30.
22. Wang W, Chen JX, Liao R, Deng Q, Zhou JJ, Huang S, Sun P. *Sequential activation of the MEK-extracellular signal-regulated kinase and MKK3/6-p38 mitogen-activated protein kinase pathways mediates oncogenic ras-induced premature senescence*. Mol Cell Biol 2002, 22: 3389–3403.
23. Gray-Schopfer VC, Cheong SC, Chong H, Chow J, Moss T, Abdel-Malek ZA, Marais R, Wynford-Thomas D, Bennett DC. *Cellular senescence in naevi and immortalization in melanoma: a role for p16?* Br J Cancer 2006, 95: 496–505.
24. Hussussian CJ, Struewing JP, Goldstein AM, Higgins PA, Ally DS, Sheahan MD, Clark WH Jr, Tucker MA, Dracopoli NC. *Germline p16 mutations in familial melanoma*. Nat Genet 1994, 8: 15–21.
25. Murphree AL, Benedict WF. *Retinoblastoma: clues to human oncogenesis*. Science 1984; 223: 1028–1033.
26. Dirac AM, Bernards R. *Reversal of senescence in mouse fibroblasts through lentiviral suppression of p53*. J Biol Chem 2003; 278: 11731–11734.
27. Kulju KS, Lehman JM. *Increased p53 protein associated with aging in human diploid fibroblasts*. Exp Cell Res 1995; 217: 336–345.

28. Herbig U, Jobling WA, Chen BPC, Chen DJ, Sedivy JM. *Telomere shortening triggers senescence of human cells through a pathway involving ATM, p53, and p21^{CIP1}, but not p16^{INK4a}*. Mol Cell 2004; 14: 501–513.
29. D’Adda di Fagagna F, Teo SH, Jackson SP. *Functional links between telomeres and proteins of the DNA-damage response*. Genes Dev 2004; 18: 1781–1799.
30. Gire V, Roux P, Wynford Thomas D, Brondello JM, Dulic V. *DNA damage checkpoint kinase Chk2 triggers replicative senescence*. EMBO J 2004; 23: 2554–2563.
31. D’Adda di Fagagna. *Living on a break: cellular senescence as a DNA-damage response* Nature, July 2008.
32. Von Zglinicki T, Saretzki G, Ladhoff J, D’Adda di Fagagna F, Jackson SP. *Human cell senescence as a DNA damage response*. Mech Ageing Dev 2005; 126: 111–117.
33. Matsuoka S, Rotman G, Ogawa A, Shiloh Y, Tamai K. *Ataxia telangiectasia-mutated phosphorylates Chk2 in vivo and in vitro*. Proc Natl Acad Sci USA 2000; 97: 10389–10394.
34. Chehab NH, Malikzay A, Appel M, Halazonetis TD. *Chk2/hCds1 functions as a DNA damage checkpoint in G1 by stabilizing p53*. Genes Dev 2000; 14: 278–288.
35. Takai H, Naka K, Okada Y, Watanabe M, Harada N, Saito S, Anderson CW, Appella E, Nakanishi M, Suzuki H, Nagashima K, Sawa H, Ikeda K. *Chk2-deficient mice exhibit radioresistance and defective p53-mediated transcription*. EMBO J 2002; 21: 5195–5205.
36. Webley K, Bond JA, Jones CJ, Blaydes JP, Craig A, Hupp T, Wynford-Thomas D. *Post-translational modifications of p53 in replicative senescence overlapping but from those induced by DNA damage*. Mol Cell Biol 2000; 20: 2803–2808.
37. Vaziri H, West MD, Allsopp RC, Davison TS, Wu YS, Arrowsmith CH, Poirier GG, Benchimol S. *ATM-dependent telomere loss in aging human diploid fibroblasts and DNA damage lead to the post-translational activation of p53 protein involving poly (ADP-ribose) polymerase*. EMBO J 1997; 16: 6018–6033.
38. Jayaraman L, Murthy KGK, Curran T, Xanthoudakis S, Prives C. *Identification of redox/repair protein Ref-1 as an activator of p53*. Genes Dev 1997; 11: 558–570.
39. Noda A, Ning Y, Venable SF, Pereira-Smith OM, Smith JR. *Cloning of senescent cell-derived inhibitors of DNA synthesis using an expression screen*. Exp Cell Res 1994; 211: 90–98.
40. Fang L, Igarashi M, Leung J, Sugrue MM, Lee SW, Aaronson SA. *p21^{Waf1/Cip1/Sdi1} induces permanent growth arrest with markers of replicative senescence in human tumor cells lacking functional p53*. Oncogene 1999; 18, 2789–2797.

41. Jeremy P. Brown, Wenyi Wei, John M Sedivy. *Bypass of Senescence after Disruption of p21^{CIP1/WAF1} Gene in Normal Diploid Human Fibroblast*. *Science* 1997; 277: 831-834
42. Harbour JW, Dean DC. *The Rb/E2F pathway: expanding roles and emerging paradigms*. *Genes Dev* 2000; 14: 2393–2409.
43. Chen QM, Bartholomew JC, Campisi J, Acosta M, Reagan JD, Ames BN. *Molecular analysis of H₂O₂-induced senescent-like growth arrest in normal human fibroblasts: p53 and Rb control G1 arrest but not cell replication*. *Biochem J* 1998; 332: 43–50.
44. Bacsı A, Woodberry M, Kruzel ML, Boldogh I. *Colostrinin delays the onset of proliferative senescence of diploid murine fibroblast cells*. *Neuropeptides* 2007; 41: 93–101.
45. J Campisi, F d'Adda di Fagagna. *Cellular senescence: when bad things happen to good cells*. *Nat Rev Mol Cell Biol* 2007; 8: 729–740.
46. Hara E, Smith R, Parry D, Tahara H, Stone S, Peters G. *Regulation of p16^{CDKN2} expression and its implications for cell immortalization and senescence*. *Mol Cell Biol* 1996; 16:859–867.
47. Herbig U, Wei W, Dutriaux A, Jobling WA, Sedivy JM. *Real-time imaging of transcriptional activation in live cells reveals rapid up-regulation of the cyclin-dependent kinase inhibitor gene CDKN1A in replicative cellular senescence*. *Aging Cell* 2003; 2:295–304.
48. Beausejour CM, Krtolica A, Galimi F, Narita M, Lowe SW, Yaswen P, Campisi J. *Reversal of human cellular senescence: Roles of the p53 and p16 pathways*. *EMBO J* 2003; 22:4212–4222.
49. Q Deng, R Liao, BL Wu, P Sun. *High intensity ras signaling induces premature senescence by activating p38 pathway in primary human fibroblasts*. *J. Biol. Chem* 2004; 279: 1050–1059.
50. JW Voncken, H Niessen, B Neufeld, U Rennefahrt, V Dahlmans, N Kubben, B Holzer, S Ludwig, UR Rapp. *MAPKAP kinase 3pK phosphorylates and regulates chromatin association of the polycomb group protein Bmi1*. *J Biol Chem* 2005; 280: 5178–5187.
51. Goldstein S, Singal DP. *Senescence of cultured human fibroblasts: mitotic versus metabolic time*. *Exp Cell Res* 1974; 88(2):359-64.
52. Hayflick LN. *The cell biology of human aging*. *Engl J Med* 1976;295(23):1302-8.
53. Harley D. *Aging and reproductive performance in langur monkeys (Presbytis entellus)*. *Am J Phys Anthropol* 1990; 83(2):253-61.

54. Holt SE, Shay JW, Wright WE. Refining the telomere-telomerase hypothesis of aging and cancer. *Nat Biotechnol* 1996; 14(7):836-9.
55. Ning Y, Xu JF, Li Y, Chavez L, Riethman HC, Lansdorp PM. *Telomere length and the expression of natural telomeric genes in human fibroblasts*. *Hum Mol Genet* 2003; 12:1329-36.
56. Gorbunova V, Seluanov A, Pereira-Smith OM. *Expression of human telomerase (hTERT) does not prevent stress-induced senescence in normal human fibroblasts but protects the cells*. *J Biol Chem* 2002; 277(41):38540-9.
57. Ulaner GA, Hu JF, Vu TH, Giudice LC, Hoffman AR. *Telomerase activity in human development is regulated by human telomerase reverse transcriptase (hTERT) transcription and by alternate splicing of hTERT transcripts*. *Cancer Res* 1998; 58:4168-72.
58. Ohmura H, Tahara H, Suzuki M, Ide T, Shimizu M, Yoshida MA. *Restoration of the cellular senescence program and repression of telomerase by human chromosome 3*. *Jpn J Cancer Res* 1995; 86:899-904.
59. Cosme-Blanco W, Shen MF, Lazar AJ, Pathak S, Lozano G, Multani AS. *Telomere dysfunction suppresses spontaneous tumorigenesis in vivo by initiating p53- dependent cellular senescence*. *EMBO Rep* 2007; 8:497-503.
60. D'Adda di Fagagna F, Reaper PM, Clay-Farrace L, Fiegler H, Carr P, Von Zglinicki T. *A DNA damage checkpoint response in telomere-initiated senescence*. *Nature* 2003; 426:194-8.
61. Wright WE, Shay JW. *The two-stage mechanism controlling cellular senescence and immortalization*. *Exp Gerontol* 1992; 27(4):383-9.
62. Sedelnikova OA, Horikawa I, Zimonjic DB, Popescu NC, Bonner WM, Barrett JC. *Senescing human cells and ageing mice accumulate DNA lesions with unrepairable double-strand breaks*. *Nat Cell Biol*. 2004; 6:168-70.
63. Dawson VL, Dawson TM. *Free radicals and neuronal cell death*. *Cell Death Differ* 1996; (1):71-8.
64. M Valko et al. *Should I stay or should I go: beta-catenin decides under stress*. *Chemico- biological interactions* 2006; 160 1-40.
65. Halliwell B, Whiteman M. *Measuring reactive species and oxidative damage in vivo and in cell culture: how should you do it and what do the results mean?* *Br J Pharmacol* 2004; 42:231-55.
66. Longo VD, Finch CE. *Evolutionary medicine: from dwarf model systems to healthy centenarians*. *Science* 2003; 299:1342-1346.

67. Kampkötter A, Volkmann TE, De Castro SH, Leiers B, Klotz LO, Johnson TE, Link CD, Henkle-Dührsen K. *Functional analysis of the glutathione S-transferase 3 from Onchocerca volvulus (Ov-GST-3): a parasite GST confers increased resistance to oxidative stress in Caenorhabditis elegans*. J Mol Biol 2003; 1: 25-37.
68. Chen Q, Fischer A, Reagan JD, Yan LJ, Ames BN. *Oxidative DNA damage and senescence of human diploid fibroblast cells*. Proc Natl Acad Sci USA 1995; 92(10):4337-41.
69. Packer L, Fuehr K. *Low oxygen concentration extends the lifespan of cultured human diploid cells*. Nature 1977; 267(5610):423-5.
70. Blander G, De Oliveira RM, Conboy CM, Haigis M, Guarente L. *Superoxide dismutase 1 knock-down induces senescence in human fibroblasts*. J Biol Chem 2003; 278(40):38966-9.
71. Iwasa H, Han J, Ishikawa F. *Mitogen-activated protein kinase p38 defines the common senescence-signalling pathway*. Genes Cells 2003; 8(2):131-44.
72. Wahl GM, Carr AM. *The evolution of diverse biological responses to DNA damage: insights from yeast and p53*. Nat Cell Biol 2001; 3(12):E277-86.
73. Andriy Marusyk, Linda J Wheeler, Christopher K. Mathews, James DeGregori. *p53 Mediates Senescence-Like Arrest Induced by Chronic Replicative Stress*. Molecular and Cellular Biology. 2007; 5336–5351.
74. Prieur A, Peeper DS. *Cellular senescence in vivo: a barrier to tumorigenesis*. Curr Opin Cell Biol 2008; 20: 150–155.
75. Jones CJ et al. *Evidence for a telomere-independent “clock” limiting RAS oncogene-driven proliferation of human thyroid epithelial cells*. Mol Cell Biol 2000; 20: 5690–5699.
76. Di Micco R et al. *Oncogene-induced senescence is a DNA damage response triggered by DNA hyper-replication*. Nature 2006; 444: 638–642.
77. Grandori C et al. *Werner syndrome protein limits MYC-induced cellular senescence*. Genes Dev 2003; 17: 1569–1574.
78. Di Micco R, Fumagalli M, D’Adda di Fagagna F. *Breaking news: high-speed race ends in arrest how oncogenes induce senescence*. Trends Cell Biol 2007; 17: 529–536.
79. Dominguez-Sola D et al. *Non-transcriptional control of DNA replication by cMyc*. Nature 2007; 448: 445–451.
80. Bartkova J et al. *Oncogene-induced senescence is part of the tumorigenesis barrier imposed by DNA damage checkpoints*. Nature 2006; 444: 633–637.

81. Rodriguez A, Griffiths-Jones S, Ashurst JL, Bradley A. *Identification of mammalian microRNA host genes and transcription units*. *Genome Res* 2004; 14:1902-1910.
82. Lee RC, Feinbaum RL, Ambros V. *The C. elegans heterochronic gene lin-4 encodes small RNAs with antisense complementarity to lin-14*. *Cell* 1993; 75: 843-854.
83. Wightman B, Ha I, Ruvkun G. *Posttranscriptional regulation of the heterochronic gene lin-14 by lin-4 mediates temporal pattern formation in C. elegans*. *Cell* 1993; 75:855-62.
84. Reinhart BJ et al. *The 21-nucleotide let-7 RNA regulates developmental timing in Caenorhabditis elegans*. *Nature* 2000, 403: 901-906.
85. Lewis BP, Burge CB, Bartel DP. *Conserved seed pairing, often flanked by adenosines, indicates that thousands of human genes are microRNA targets*. *Cell* 2005; 120:15-20
86. Ketting RF, Fischer SE, Bernstein E, Sijen T, Hannon GJ, Plasterk RH. *Dicer functions in RNA interference and in synthesis of small RNA involved in developmental timing in C. elegans*. *Genes Dev* 2001; 15(20):2654-9.
87. Ge XQ, Jackson DA, Blow JJ. *Dormant origins licensed by excess Mcm2-7 are required for human cells to survive replicative stress*. *Genes Dev* 2007; 21: 3331-3341.
88. Altuvia Y, Landgraf P, Lithwick G, Elefant N, Pfeffer S, Aravin A, et al. *Clustering and conservation patterns of human microRNAs*. *Nucleic Acids Res* 2005; 33:2697-2706.
89. Lee Y, Kim M, Han J, Yeom KH, Lee S, Baek SH et al. *MicroRNA genes are transcribed by RNA polymerase II*. *EMBO J* 2004; 23:4051-4060.
90. Denli AM, Tops BB, Plasterk RH, Ketting RF, Hannon GJ. *Processing of primary microRNAs by the Microprocessor complex*. *Nature* 2004; 432(7014):231-5.
91. Gregory RI, Yan KP, Amuthan G, Chendrimada T, Doratotaj B, Cooch N, Shiekhattar R. *The Microprocessor complex mediates the genesis of microRNAs*. *Nature* 2004; 432(7014):235-40.
92. Bohnsack MT, Czaplinski K, Gorlich D. *Exportin 5 is a RanGTP-dependent dsRNA-binding protein that mediates nuclear export of pre-miRNAs*. *RNA* 2004; 10(2):185-91.
93. Lund AH, Van Lohuizen M. Polycomb complexes and silencing mechanisms. *Curr Opin Cell Biol* 2004; 16(3):239-46.
94. Gregory RI, Chendrimada TP, Cooch N, Shiekhattar R. Human RISC couples microRNA biogenesis and posttranscriptional gene silencing. *Cell* 2005; 123(4):631-40.
95. Maniataki E, Mourelatos Z. *A human, ATP-independent, RISC assembly machine fueled by pre-miRNA*. *Genes Dev* 2005; 19(24):2979-90.

96. Schwarz DS, Hutvagner G, Du T, Xu Z, Aronin N, Zamore PD. *Asymmetry in the assembly of the RNAi enzyme complex*. Cell 2003; 115(2):199-208.
97. Hutvagner G, Zamore PD. *A microRNA in a multiple-turnover RNAi enzyme complex*. Science 2002; 297(5589):2056-60.
98. Martinez J, Tuschl T. *RISC is a 5' phosphomonoester-producing RNA endonuclease*. Genes Dev 2004; 18(9):975-80.
99. Humphreys DT, Westman BJ, Martin DI, Preiss T. *MicroRNAs control translation initiation by inhibiting eukaryotic initiation factor 4E/cap and poly(A) tail function*. Proc Natl Acad Sci USA 2005; 102(47):16961-6.
100. Maroney PA, Yu Y, Nilsen TW. *MicroRNAs, mRNAs, and translation*. Cold Spring Harb Symp Quant Biol 2006; 71:531-5.
101. Nottrott S, Simard MJ, Richter JD. *Human let-7a miRNA blocks protein production on actively translating polyribosomes*. Nat Struct Mol Biol 2006; 13(12):1108-14.
102. Pillai RS, Bhattacharyya SN, Artus CG, Zoller T, Cougot N, Basyuk E, Bertrand E, Filipowicz W. *Inhibition of translational initiation by Let-7 MicroRNA in human cells*. Science 2005; 309(5740):1573-6.
103. Sen GL, Blau HM. *Argonaute 2/RISC resides in sites of mammalian mRNA decay known as cytoplasmic bodies*. Nat Cell Biol 2005; 7(6):633-6.
104. Behm-Ansant I, Rehwinkel J, Izaurralde E. *MicroRNAs silence gene expression by repressing protein expression and/or by promoting mRNA decay*. Cold Spring Harb Symp Quant Biol 2006; 71:523-30.
105. Chu CY, Rana TM. *Translation repression in human cells by microRNA-induced gene silencing requires RCK/p54*. PLoS Biol. 2006; 4(7):e210.
106. Standart N, Jackson RJ. *MicroRNAs repress translation of m7Gppp-capped target mRNAs in vitro by inhibiting initiation and promoting deadenylation*. Genes Dev 2007; 21(16):1975-82.
107. Bhattacharyya SN, Habermacher R, Martine U, Closs EI, Filipowicz W. *Stress-induced reversal of microRNA repression and mRNA P-body localization in human cells*. Cold Spring Harb Symp Quant Biol 2006; 71:513-21.
108. Lee RC, Feinbaum RL, Ambros V. *The C. Elegans heterochronic gene lin-4 encodes small RNAs with antisense complementarity to lin-14*. Cell 1993; 3: 843-54.
109. Fango Cao, Xiangzhi Li, Samantha Hiew, Hugh Brady, Yifan Liu, Yali Dou. *Dicer independent small RNAs associate with telomeric heterochromatin*. Advanced 2009; 15: 1274-1281.

110. Chivukula RR, Mendell JT. *Circular reasoning: microRNAs and cell-cycle control*. Trends Biochem Sci 2008; 33(10):474-81.
111. De Stanchina, ZY Xuan, Y Liang, W Xue et al. *A microRNA component of p53 tumor suppressor network*. Nature 2007; 477: 1130-U16.
112. L Polisenò, L Pitto, M Simili, L Mariani, L Riccardi, A Ciucci, M Rizzo, M Evangelist, A Mercatanti, PP Pandolfi, G Rainaldi. *The proto-oncogene Lrf is under post-transcriptional control of Mir-20a: Implications for senescence*. Plos ONE 2008; 3:2542.
113. Bhaumik D, Patil CK, Campisi J. *MicroRNAs: an important player in maintaining a balance between inflammation and tumor suppression*. Cell Cycle 2009; 8(12):1822.
114. Grillari J., Hackl M. Grillari-Voglauer R. *miR17-92 clusters: ups and downs in cancers and aging*. Biogerontology, 2010; 11 (4): 501-506
115. Methods Enzymol. 2002, 397: 253-257
116. Yoshimura et al. *Vertebrate POLQ and POL β cooperate in base excision repair of oxidative DNA Damage*. Mol. Cell. 2006; 24 (1): 115-125
- 117 Sugasawa K. *DNA repair pathways involving Cul4a ubiquitin ligases*. Tanpakushitsu Kakusan Koso 2006; 51: 1339-44
- 118 Stephen Y. Chan, Ying-Yi Zhang, Craig Hemann, Christopher E. Mahoney, Jay L. Zweier, and Joseph Loscalzo. *MicroRNA-210 Controls Mitochondrial Metabolism during Hypoxia by Repressing the Iron-Sulfur Cluster Assembly Proteins ISCU1/2*. Cell Metab. 2009; 10(4): 273–284

Hakuna Matata.